Dalton Transactions

From the Parent Phosphinidene-Carbene Adduct NHC=PH to Cationic P4-Rings and P2-Cycloaddition Products

Journal:	*Dalton Transactions*
Manuscript ID	DT-ART-08-2015-003014.R1
Article Type:	Paper
Date Submitted by the Author:	10-Sep-2015
Complete List of Authors:	Grützmacher, Hansjörg; ETH Honggerberg, Department of Chemistry Gilliard, Robert; ETH, Chemistry Beil, Andreas; ETH, Chemistry

SCHOLARONE™
Manuscripts

From the Parent Phosphinidene-Carbene Adduct NHC=PH to Cationic P_4-Rings and P_2-Cycloaddition Products

Andreas Beil,[a] *Robert J. Gilliard, Jr.,*[a] *Hansjörg Grützmacher*[a]*

[a] Laboratory of Inorganic Chemistry, ETH Zürich, Vladimir-Prelog-Weg 1, 8093 Zürich, Switzerland.
E-mail: hgruetzmacher@ethz.ch

CCDC numbers: 1415566-1415574

Abstract

Reactions of the parent phosphinidene-carbene adduct ^{Dipp}NHC=PH with chlorophosphanes are reported herein. The obtained ^{Dipp}NHC-substituted chlorodiphosphanes, ^{Dipp}NHC=P-PClR, and the formation of their cationic derivatives, [^{Dipp}NHC-P=PR]$^+$, were also explored. Depending on the steric demand of their substituents, these cations were found to be monomeric [^{Dipp}NHC-PP-N^{i}Pr$_2$][GaCl$_4$] or to dimerise to cyclotetraphosphanes [^{Dipp}NHC-PP-R]$_2$[GaCl$_4$]$_2$ (R = Ph, NMe$_2$). For R = NMe$_2$, this dication is the first isolated example of a tetrasubstituted all-σ^3 cyclotetraphosphane. Finally, the hetero-Diels-Alder reactivity of these cations was studied with 2,3-dimethylbuta-1,3-diene and cyclopentadiene, resulting in the isolation of a number of cationic 1,2-diphosphinanes.

Introduction

Since the first preparation of stable carbenes,[1, 2] they have been used extensively to facilitate the isolation of a large number of previously inaccessible compounds.[3-7] Specifically, N-heterocyclic carbenes (NHCs) stabilise low coordinate species of many main group elements,[8-11] among them phosphorus.[2, 12-14]

Figure 1 depicts a selection of NHC-supported phosphorus-containing compounds described in the literature. The neutral diphosphorus compound ^{Dipp}NHC-PP-^{Dipp}NHC (**A**) was obtained by Robinson *et al.* in 2008 from reduction of the ^{Dipp}NHC-PCl$_3$ adduct with KC$_8$ (^{Dipp}NHC =

1,3-bis(2,6-diisopropylphenyl)imidazole-2-ylidene).[12, 13] Bertrand *et al.* oxidized **A** with FcOTf (Fc = ferrocenium, OTf = triflate) to obtain the dication [^{Dipp}NHC-PP-^{Dipp}NHC]$^{2+}$ (**B**).[15] In a similar synthesis, Weigand and co-workers isolated the chlorinated species **C** from ^{Dipp}NHC-PCl$_2$(OTf) by reducing the cationic adduct with sodium.[16, 17]

The diphosphenyl phosphonium **D** is an example of a structure containing P-P multiple bonds which is stabilised by steric shielding.[18] It was obtained from the reaction of 1-amino-2-aryldiphosphene [H$_2$(^{t}Bu)$_3$C$_6$-P=P-NR$_2$]) and PPh$_3$ in the presence of CF$_3$SO$_3$H.

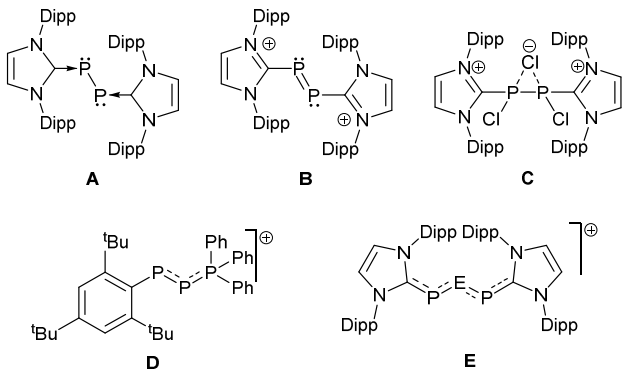

Figure 1 Selected NHC-stabilised phosphorus species (**A-C, E**, E = P, As)[12, 15-17, 19] and diphosphenyl phosphonium **D**[18]

The parent phosphinidene-carbene adduct ^{Dipp}NHC=PH **1** (see Scheme 1) was published by Driess and co-workers, who prepared it from a phosphasilene and the respective NHC.[20] A lithiated derivative of **1** was reported by Robinson *et al.* in 2010.[12, 13] Recently, our group reported facile syntheses of **1** from sodium phosphaethynolate, Na(OCP) or P$_7$(SiMe$_3$)$_3$ in good yields.[19] An additional synthesis of **1** has been reported by Tamm *et al.* via solvolysis of ^{Dipp}NHC=PSiMe$_3$ with methanol.[21] In addition, we described a synthesis of the saturated NHC analogue of **1**, ^{Dipp}NHC*=PH (^{Dipp}NHC* = 1,3-bis(2,6-diisopropylphenyl)-4,5-dihydro-imidazole-2-ylidene) from the respective imidazolium salt and PH$_3$, forming [^{Dipp}NHC*-H]-[PH$_2$]. This subsequently undergoes dehydrogenation with *o*-quinone to form the phosphinidene.[22] The adduct **1** has been applied as a building block for the synthesis of NHC-stabilised tripnictogen cations [(^{Dipp}NHC)$_2$(μ-PEP)][Cl] (E = P, As) which were simply obtained by mixing two equivalents of **1** with ECl$_3$ in the presence of a base (**E**, Figure 1).[20] This reaction proceeds under spontaneous dissociation of the P-Cl bond to give the cation **E** and a Cl$^-$ counter anion. In complexes of ruthenium and rhodium, **1** was found to be a tightly bound ligand.[21] Bertrand and co-workers reported the synthesis of the parent phosphenium-carbene adduct [NHC-PH$_2$]$^+$ from a very bulky NHC=PH and CF$_3$SO$_3$H.[23] In combination,

these experiments show that NHC-phosphinidene adducts are strong electron donors supporting the assumption that the ylidic resonance structure NHC^{+}-PR^{-} is a strong contributor to the electronic ground state.

Results and Discussion

To further elucidate the synthetic potential of ^{Dipp}NHC=PH (**1**) for the synthesis of new phosphorus-containing molecules, we studied the reactivity towards chloro- and dichloro-phosphanes.

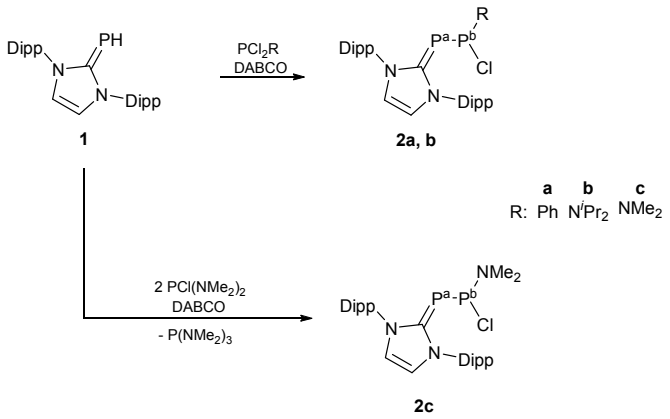

Scheme 1 Synthesis of ^{Dipp}NHC-chlorodiphosphanes **2a-c** from parent phosphinidene-carbene adduct **1**

The parent phosphinidene-carbene adduct ^{Dipp}NHC=PH (**1**) exhibits P-nucleophilic character and reacts with dichlorophosphanes PCl_2R in the presence of DABCO (1,4-diazabicyclo[2.2.2]octane) as a non-nucleophilic base to yield neutral species of type ^{Dipp}NHC-PPClR, R = Ph (**2a**) or N^iPr_2 (**2b**) (Scheme 1).

In a similar reaction, **1** reacts with chlorobis(dimethylamino)phosphane in the presence of DABCO (Scheme 1). However, the expected diphosphane, ^{Dipp}NHC=P-P$(NMe_2)_2$, was not observed but a second equivalent of $PCl(NMe_2)_2$ acts as chloride donor yielding ^{Dipp}NHC-PPClNMe_2 (**2c**) and $P(NMe_2)_3$.

Complete conversion was observed in ^{31}P NMR and the products can be isolated as microcrystalline materials via hexane extraction of the crude reaction mixtures. Table 1 lists the ^{31}P NMR shifts of the reported species. For the carbene-stabilised chlorodiphosphanes, ^{31}P NMR spectra show two strongly coupled doublets of an AB-spin system with average $^{1}J_{PP}$ =

376 (**2a**), 337 Hz (**2b**) and 350 Hz (**2c**). The chemical shift of the phosphorus atoms P^a adjacent to the carbene centre are similar [-17.3 ppm (**2a**), -16.7 ppm (**2b**) and -33.5 ppm (**2c**)]. In notable contrast, the chemical shift for P^b strongly differs between the phenyl-substituted species **2a** (157.6 ppm) and the amino-substituted derivatives of **2b** (213.0 ppm) and **2c** (214.1 ppm) (Scheme 1). The downfield shift of the latter might be explained by the presence of the electronegative amino substituents in **2b** and **2c**. The values for P^a (-17.3 to -33.5 ppm) are in agreement with other carbene-phosphinidene adducts such as ^{Dipp}NHC=PPh with $\delta(^{31}P)$ = -18.9 ppm.[24]

The molecular structures of **2a** and **2b** are shown in Figure 2 and Figure 3, respectively.[25] Table 2 lists selected structural parameters of the reported products. All structural parameters discussed herein are based on single-crystal X-ray diffraction experiments.[26] The P-P distances in **2a** (2.13 Å) and **2b** (2.15 Å) are shorter than a P-P single bond (2.20 Å).[27, 28] Interestingly, the P2-Cl distances in **2a** (2.17 Å) and **2b** (2.25 Å) are remarkably longer than the sum of the covalent radii (2.04 Å)[28] and other P-Cl distances found in solid aryl-substituted chlorophosphanes, e.g. $(2,6\text{-}(CF_3)_2H_3C_6)_2PCl$ (2.07 Å)[29] and $(2,4,6\text{-}(CF_3)_3H_2C_6)_2PCl$ (2.06 Å).[30] Also, a comparable dicationic bis-NHC-supported chlorophosphane $[(NHC)_2PCl]^{2+}$ reported by Weigand *et al.* shows a P-Cl distance of 2.04 Å.[31] Finally, the bond lengths to the third substituent at P2 [d(P2-C28) = 1.84 Å (**2a**) and d(P2-N3) = 1.66 Å (**2b**)] are shorter than normal single bonds (1.87 Å and 1.76 Å, respectively).[28] These findings suggest that the P2-Cl bonds in **2a** and **2b** are weak and that the bonds in the carbene-P-P-R moieties have partial double bond character.

In both structures, the P2 atom is in a trigonal pyramidal environment with angle sums of 301.90 ° (**2a**) and 304.11 ° (**2b**). This compares very well with data observed in the dication $[(NHC)_2PCl]^{2+}$ ($\Sigma°(P)$ = 308.86°),[31] $(2,6\text{-}(CF_3)_2H_3C_6)_2PCl$ ($\Sigma°(P)$ = 306.38°),[32] and $(2,4,6\text{-}(CF_3)_3H_2C_6)_2PCl$ ($\Sigma°(P)$ = 306.49°).[30]

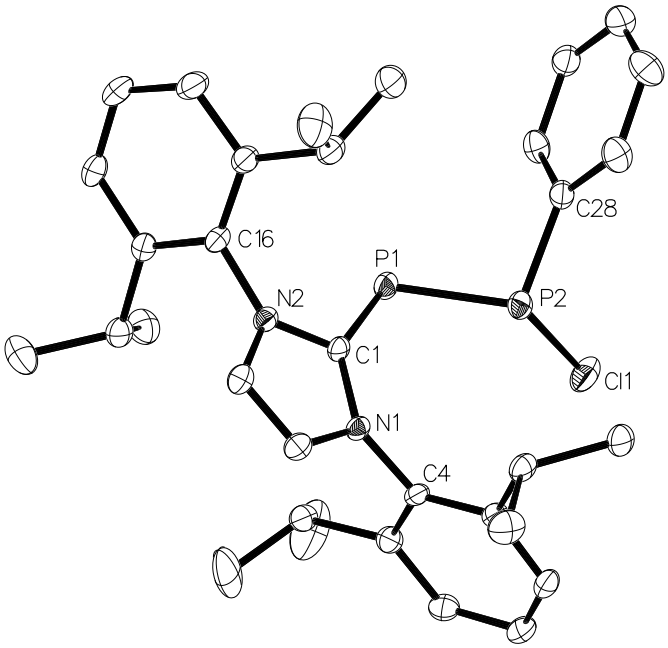

Figure 2 Molecular structure of **2a** (thermal ellipsoids at 50 % probability, H atoms are omitted for clarity). Selected bond distances (Å), angles and torsion angles (°): C1-P1 1.8017(18), P1-P2 2.1254(6), P2-Cl1 2.1656(7), P2-C28 1.8384(19), C1-P1-P2 96.35(6), P1-P2-Cl1 107.72(3), P1-P2-C28 97.99(6), Cl1-P2-C28 96.19(6), C1-P1-P2-C28 -142.46. Angle sum at P2 301.90 °

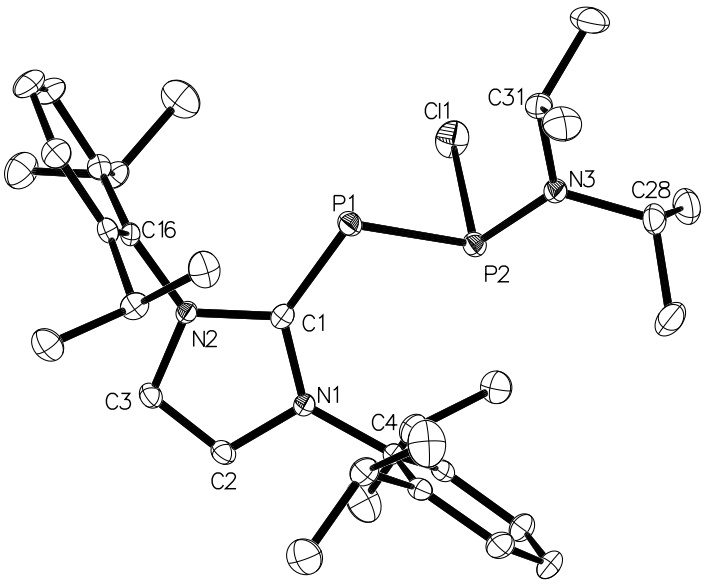

Figure 3 Molecular structure of **2b** (thermal ellipsoids at 50 % probability, H atoms are omitted for clarity). Selected bond distances (Å), angles and torsion angles (°): C1-P1 1.7835(16), P1-P2 2.1518(6), P2-Cl1 2.2474(6), P2-N3 1.6604(14), C1-P1-P2 97.14(5), P1-P2-Cl1 100.90(2), P1-P2-N3 102.04(5), Cl1-P2-N3 101.17(5), C1-P1-P2-N3 159.86. Angle sum at P2 304.11 °

Table 1 ^{31}P NMR shifts of the reported products

δ(^{31}P)/ ppm	**2a**	**2b**	**2c**	**(3a)$_2$**	**3b**	**(3c)$_2$**	**4a**	**4b**	**4c**	**5a**	**5b**	**5b'**	**5c**
1	157.6	215.1	214.1	-24.2	492.1	16.6	-19.4	32.9	65.4	-13.0	42.5	35.7	66.5
2	-17.3	-18.4	-33.5	-69.3	158.1	-6.9	-44.7	-56.5	-41.2	-15.1	-24.3	-19.0	-25.2
Multi-plicity	2	2	2	3	2	3	2	2	2	2	2	2	2
Solvent	THF-d$_8$	THF-d$_8$	THF-d$_8$	THF-d$_8$	THF-d$_8$	THF-d$_8$	$CDCl_3$	$CDCl_3$	$CDCl_3$	THF-d$_8$	THF	THF	$CDCl_3$

Table 2 Selected bond distances (Å) and angles (°) of the described compounds. X = C28 for **a** and N3 for **b** and **c**, Y = Cl for **2a**, **2b** and **2c**, Y = Cn and Z = Cm for the cycloaddition products **4a-4c**, **5a** and **5c**

	2a	**2b**	**3b**	**4a**	**4b**	**4c**	**5a**	**5c**
C1-P1	1.8017(18)	1.7835(16)	1.821(2)	1.8506(17)	1.844(2)	1.8448(18)	1.8501(17)	1.850(3)
P1-P2	2.1254(6)	2.1518(6)	2.0611(7)	2.2312(6)	2.2285(8)	2.2204(7)	2.2343(6)	2.2623(10)
P2-X	1.8384(19)	1.6604(14)	1.6411(17)	1.8406(18)	1.6790(19)	1.6899(18)	1.828(2)	1.678(3)
P2-Y	2.1656(7)	2.2474(6)	-	1.8667(18)	1.873(2)	1.879(2)	1.900(2)	1.895(3)
P1-Z	-	-	-	1.8695(18)	1.854(2)	1.8761(18)	1.8920(19)	1.895(3)
C1-P1-P2	96.35(6)	97.14(5)	94.32(6)	98.52(6)	102.76(7)	103.00(6)	96.89(5)	99.55(8)
C1-P1-Z	-	-	-	104.32(8)	103.59(9)	106.26(8)	106.60(8)	107.53(13)
P1-P2-X	97.99(6)	102.04(5)	105.66(6)	100.56(6)	101.88(7)	99.07(6)	103.24(7)	102.12(9)
P1-P2-Y	107.72(3)	100.90(2)	-	96.97(6)	95.38(8)	95.66(7)	89.82(7)	88.56(9)

Treating **2a-c** with the Lewis acidic gallium trichloride at ambient temperature led to chloride abstraction and the formation of the respective cations **(3a)$_2$** (R = Ph), **3b** (R = N^{i}Pr$_2$) and **(3c)$_2$** (R = NMe$_2$). In these cationic species, the presence of different substituents (R = Ph, N^{i}Pr$_2$ or NMe$_2$) results in the formation of two topologies in the products (Scheme 2). While cation **3b** remains monomeric, the cations of **2a** and **2c** dimerise in a [2+2] cycloaddition reaction yielding symmetrically substituted dicationic P_4 rings. The cations **3b** and **(3c)$_2$** have been isolated as crystalline materials and characterised by single crystal X-ray crystallography. While **(3a)$_2$** has not been isolated, the structure is assigned based on NMR

and mass spectrometry data. Specifically, the dimeric structure of **(3a)$_2$** is evident on the basis of the ^{31}P NMR spectrum (obtained when a solution of **2a** is reacted with $GaCl_3$) which shows an A_2B_2 ^{31}P spin system consisting of two coupled triplets (J = 112 Hz) with equivalent signal intensity at chemical shifts of -24.2 and -69.3 ppm. This postulation is supported by MALDI-TOF mass spectra showing a strong signal for the ion $[^{Dipp}NHC\text{-}P(PPh)_2]^+$ ($C_{39}H_{46}N_2P_3^+$, m/z (calc.) = 635.2874, m/z (found) = 635.2869, see SI for NMR and mass spectra).

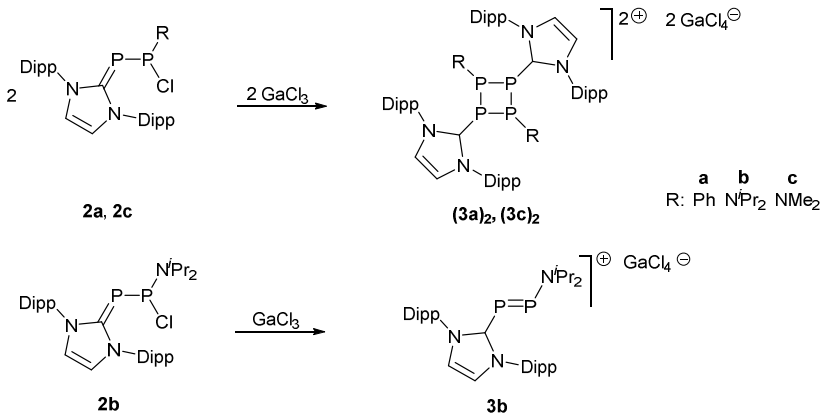

Scheme 2 Chloride abstraction from **2a-c** via reaction with $GaCl_3$ yielding cationic species. The diisopropylamino substituted derivative **3b** remains monomeric, while the other derivatives form dimeric structures. The dimeric structure of **(3a)$_2$** has been assigned based on ^{31}P NMR and MS data

The respective dimethylamino derivative **(3c)$_2$** has been crystallised as tetrachloridogallate with one equivalent of 1,2-dimethoxyethane (Figure 4). The structure shows a symmetrically substituted butterfly-like P_4 ring with average P-P distances of 2.26 Å, which is slightly longer than a P-P single bond (2.20 Å),[28] possibly due to steric reasons. The average P-P-P angle at the carbene-substituted phosphorus atom is 86.0 °, while the average P-P-P angle at the phosphorus bearing the smaller, electronegative amino unit is 78.0 °. The nitrogen centres of the dimethylamino moieties are in an almost planar coordination sphere with angle sums of Σ°(N) = 359.85° at N3 and Σ°(N) = 358.47° at N6 indicating sp^2 hybridisation, i.e. a delocalisation of the free electron pair of these nitrogen atoms to the adjacent phosphorus atoms. Furthermore, the P-N distances of 1.66 Å are between values for P-N single (1.76 Å) and double (1.52 Å) bonds.[28] The ^{31}P NMR spectrum of **(3c)$_2$** shows two coupled triplets (J = 163 Hz) at chemical shifts of 16.6 and -6.9 ppm. The downfield shift of these signals compared to those of **(3a)$_2$** (-24.2 and -69.3 ppm) are likely caused by the higher group

electronegativity of the amino substituent in **(3c)$_2$** when compared to the phenyl substituent in **(3a)$_2$**.

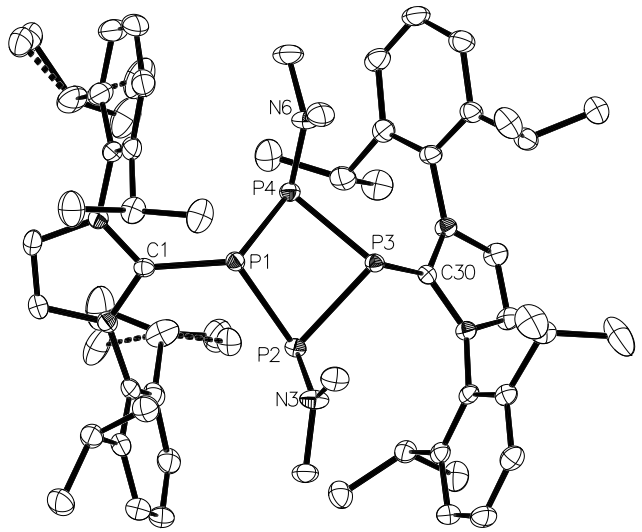

Figure 4 Molecular structure of **(3c)$_2$** (thermal ellipsoids at 50 % probability, H atoms, disordered counterions and the cocrystallised DME molecule are omitted for clarity). Selected bond distances (Å) and angles (°): C1-P1 1.8348(18), C30-P3 1.8278(18), P1-P2 2.2597(7), P3-P4 2.2489(7), P1-P4 2.2575(7), P3-P2 2.2668(7), P2-N3 1.6576(17), P4-N6 1.6639(17), P1-P2-P3 77.82(2), P3-P4-P1 78.23(2), P4-P1-P2 85.99(2), P4-P3-P2 86.03(2). Angle sum at N3 359.85° and N6 358.47°

To the best of our knowledge, **(3c)$_2$** is the first isolated example for a cationic tetrasubstituted all-σ^3 cyclotetraphosphane. Figure 5 shows selected examples of P_4 ring systems reported in the literature. Besides neutral, saturated cyclotetraphosphanes like $(PCy)_4$[33, 34] (Cy = cyclohexyl) or $(PPh)_4$,[35, 36] or products with all-σ^3 coordination (e.g. butterfly-shaped $(Mes^*PPCl)_2$ (Mes* = 2,4,6-(^{t}Bu)$_3$H$_2$C$_6$)[37]), comparable compounds such as the N-substituted cyclotetraphosphane **F** reported by Frank *et al.* are neutral and exhibit a mixed σ^4-σ^2 coordination.[38] Furthermore, there are also examples of neutral disubstituted all-σ^3 P_4 ring systems bearing a transannular P-P bond (*cf.* example **G**).[39, 40] With P-P distances around 2.23 Å and average P-P-P angles of 84.5 °, the structural parameters of the butterfly-shaped $(PCy)_4$[33, 34] and $(PPh)_4$[35, 36] are comparable with those of **(3c)$_2$** with an average P-P distance of 2.26 Å and an average P2-P1/P3-P4 angle of 86.0 °.

Other cationic or dicationic examples of P_4 ring systems exhibit either a $(\sigma^3)_3$-σ^4 (example **H**) or a $(\sigma^3)_2$-$(\sigma^4)_2$ coordination (example **I**), respectively, where one or two phosphorous atoms are quarternised.[41-49] Finally, there are examples for bicyclic cationic species with transannular P-P bonds like the dicationic all-σ^3 structures $[Ph_3EPP]_2^{2+}$ (E = P, As, *cf.* **J**)

reported by Weigand *et al.*[50] The cationic P_4 ring systems with $(\sigma^3)_3$-σ^4 coordination was recently reported by Schulz and co-workers (example **K**).[51]

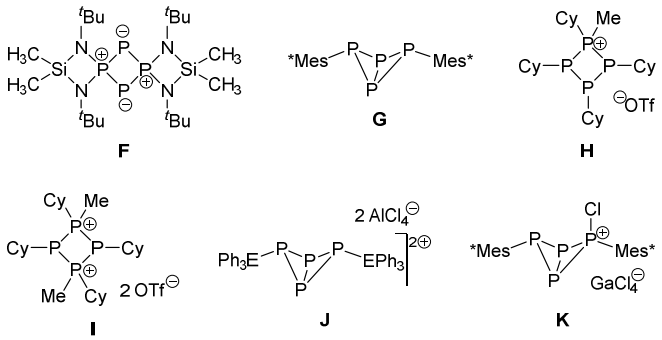

Figure 5 Selected examples of neutral, cationic and dicationic P_4 ring systems. E = P, As[38-51]

For the cationic species **3b**, the ^{31}P NMR spectrum shows two coupled doublets (J = 525 Hz) at chemical shifts of 492.1 and 158.1 ppm. Both shifts are similar to the data reported for $[(^{Dipp}NHC)_2(\mu\text{-}P_3)][Cl]$ (591.9 and 190.6 ppm, **E** in Figure 1).[19] The high frequency resonance also compares well to the ^{31}P shift of the symmetric $[^{Dipp}NHC\text{-}PP\text{-}^{Dipp}NHC]^{2+}$ dication (452.0 ppm, **B**) reported by Bertrand and coworkers.[15]

In the molecular structure of **3b** (Figure 6) the P-P distance of 2.06 Å is similar to the P-P distance reported for the symmetric $[^{Dipp}NHC\text{-}PP\text{-}^{Dipp}NHC]^{2+}$ (2.08 Å, **B**) and slightly longer than other reported P-P double bond distances (1.95 – 2.04 Å),[52] e.g. compound **D** (2.03 Å).[18] The average P-P distance in the symmetric $[(^{Dipp}NHC)_2(\mu\text{-}P_3)][Cl]$ (**E**) is 2.09 Å, indicating the delocalisation of the π-bond between two P-P-units.[19] The P-N distance in **3b** (1.64 Å) is significantly shorter than a P-N single bond (1.76 Å)[28] accounting for partial double bond character. This is further supported by the angle sum at N3 (Σ°(N) = 359.59°) suggesting an allyl anion-like 4π electron interaction in the P-P-NR_2 group. A P-N bond of comparable lengths was observed in the cationic amino phosphaalkene, Ph_3P^+-CH=P-N^{i}Pr$_2$ (1.62 Å), which likewise contains a planar conjugated 4π C-P-NR_2 unit.[53]

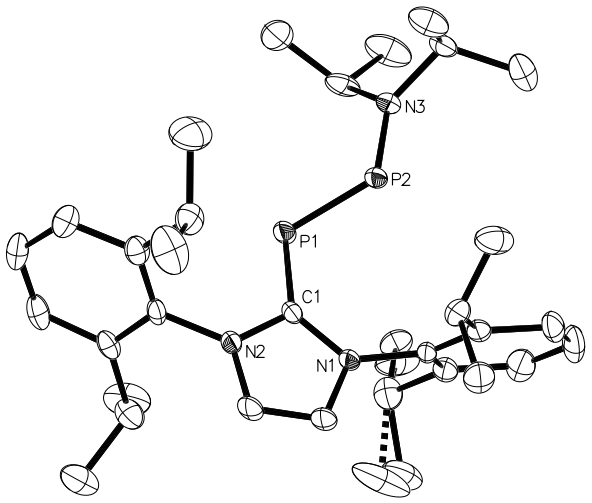

Figure 6 Molecular structure of **3b** (thermal ellipsoids at 50 % probability, H atoms are omitted for clarity). Selected bond distances (Å) and angles (°): C1-P1 1.821(2), P1-P2 2.0611(7), P2-N3 1.6411(17), C1-P1-P2 94.32(6), P1-P2-N3 105.66(6). Angle sum at N3 359.59 °

The cationic derivatives of the chlorodiphosphane carbene adducts **2a-c** readily undergo [4+2] Diels-Alder cycloaddition reactions with 2,3-dimethyl-1,3-butadiene (DMB) yielding the cationic 1,2-diphosphinanes **4a-c** (Scheme 3). These experiments clearly indicate the double bond character of the P-P-bonds in $[^{Dipp}NHC\text{-}P{=}P\text{-}R]^+$. Similar reactions have been shown by Cummins *et al.* by transferring *in situ* generated molecular P_2 to conjugated dienes[54] and Schulz and coworkers, who were able to show the presence of a P-P double bond in $[(Mes^*P)_2PPCl]^+$ by trapping this highly reactive intermediate with DMB.[51]

Regarding **2a** and **2c**, the chloride abstraction must be performed in presence of the diene to trap the *in situ* formed cations **3a** or **3c**, respectively, to avoid the formation of dimers **(3a)$_2$** and **(3c)$_2$**, which are inaccessible for cycloaddition reactions at ambient temperature. Alternatively, the [4+2] cycloaddition product **4c** is quantitatively obtained upon heating **(3c)$_2$** in the presence of 2,3-dimethylbuta-1,3-diene to 60 °C. This experiment shows that the monomeric cation **3c** exists at elevated temperatures and can be trapped by DMB (*cf.* SI for NMR experiment). Figure 7, Figure 8 and Figure 9 show the molecular structures of the cationic cycloadducts **4a-c**.

The reactivity towards cyclopentadiene is determined by the steric properties of the substituents, as observed for the dimerisation: The chloride abstraction from **2a** and **2c**, bearing the less bulky phenyl and dimethylamino moieties, in presence of cyclopentadiene

yields the *exo*-cycloadducts[55] **5a** and **5c**, which crystallise as tetrachloridogallates (see Figure 10 and Figure 11).

In contrast, the reaction of the bulkier cationic diisopropylamino derivative **3b** with cyclopentadiene leads to the formation of the putative diastereomeric cycloadducts **5b** and **5b'**, in approximately 1:3 ratio (Scheme 3). After 12 h at room temperature, the product ratio changes to approximately 1:1, meaning that product **5b'** is converted into **5b**. Hence, we assume that **5b'** is the kinetic reaction product while **5b** is the thermodynamic product. Based on the structures of crystalline **5a** and **5c** we assume that the thermodynamically more stable isomer **5b** has an *exo*-configuration while we assign an *endo*-configuration to **5b'**. Evaporating the reaction mixture *in vacuo* leads to the formation of **3b** in a cycloreversion reaction. All attempts to crystallise the products from the reaction mixture led to the isolation of **3b** and we were not able to isolate **5b'** or **5b** (see SI for ^{31}P NMR spectra). The reversibility of the reaction is also supported by the facile isomerisation of the cycloadducts observed in ^{31}P NMR.

Even though **5c** has been isolated in crystalline form, it is very sensitive when kept under vacuum. In a sample of **5c**, which has been exposed to vacuum, not only are traces of dimeric **(3c)$_2$** observed in the ^{31}P NMR spectrum, but also two weak doublets with chemical shifts of 495.6 and 160.5 ppm (J = 521 Hz). These are assigned to the monomeric cation **3c** (*cf.* the shifts of **3b** of 492.1 and 158.1 ppm, see SI for ^{31}P NMR spectrum). This result indicates that the dimethylamino-substituted species displays reactivity between the phenyl-substituted compound and the diisopropylamino derivative and that an amino group electronically stabilizes a cationic NHC substituted diphosphene.

Selected structural parameters of the isolated cycloaddition products **4a-c** and **5a** and **5c** are listed in Table 2. All bond lengths and angles are within the expected range. The C1-P1 distances (1.84-1.86 Å) are slightly shorter than the P2-C distances (1.87 – 1.90 Å) indicating some backbonding into the NHC group. The P-P distances (2.23 Å) are within the range observed for P-P single bonds (sum of the covalent radii = 2.20 Å)[28] and correspond well to a highly fluorinated crystalline example of a 1,2-diphosphinane described by Grobe and co-workers (P-P = 2.22 Å).[56]

For C-substituted 1,2-diphosphinanes, ^{31}P NMR shifts are reported in the range between 0 and -50 ppm.[57-59] These values correlate with the shifts found for the P-atoms in **4a** (-19.4 ppm) and **5a** (-13.0 ppm) bearing phenyl substituents. The ^{31}P signals of the N-substituted

derivatives **4b**,**c** and **5b**,**c** are again shifted to higher frequencies ("downfield") at values between 32.9 and 66.5 ppm, as expected for atoms bearing electronegative substituents.

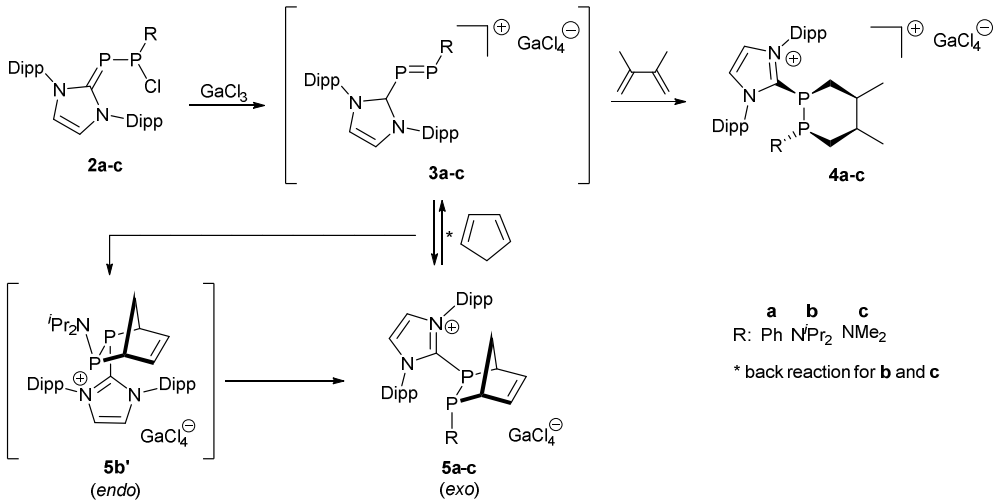

Scheme 3 The cycloaddition reactivity of cations **3a-c** towards 2,3-dimethylbuta-1,3-dien (DMB) and 1,3-cyclopentadiene (CPD). For the reaction with CPD, only *exo*-isomers **5a** and **5c** have been isolated. For the diisopropylamino derivative both the *endo*- and the *exo*-isomer are observed in ^{31}P NMR, while an isomerisation from **5b'** to **5b** is observed. *) The application of vacuum on **5b** and **5c** leads to the back formation of the cationic species **3b** and **3c** or the respective dimer **(3c)$_2$**, while **5a** is stable against vacuum. For the proof of reversibility and ^{31}P NMR spectra *cf.* SI

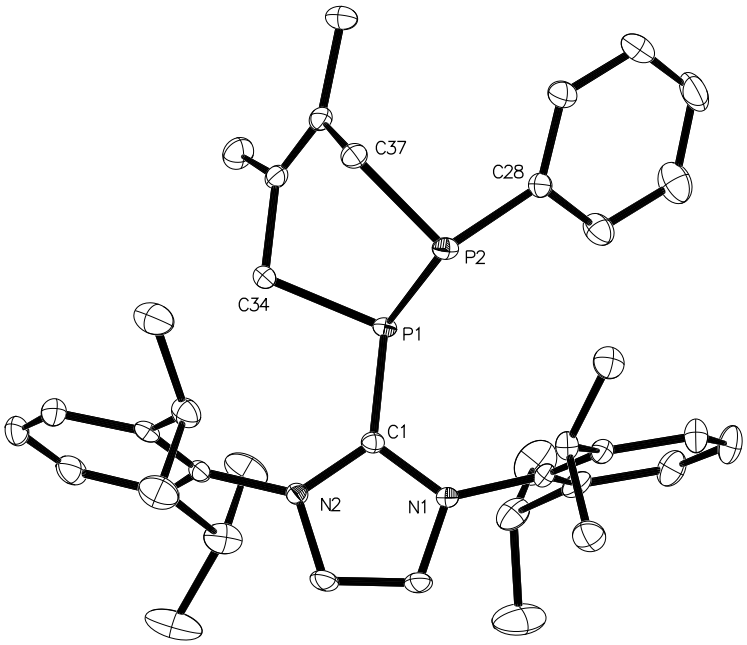

Figure 7 Molecular structure of **4a** (thermal ellipsoids at 50 % probability, H atoms are omitted for clarity). Selected bond distances (Å) and angles (°): C1-P1 1.8506(17), P1-P2 2.2312(6), P2-C28 1.8406(18), P1-C34 1.8695(18), P2-C37 1.8667(18), C1-P1-P2 98.52(6), C1-P1-C34 104.32(8), P1-P2-C28 100.56(6)

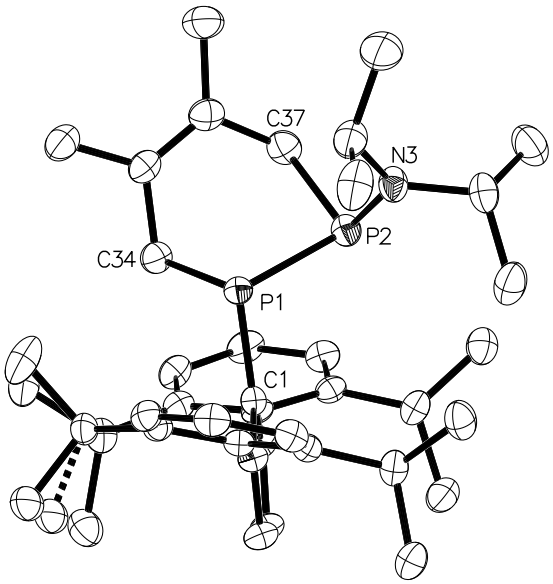

Figure 8 Molecular structure of **4b** (thermal ellipsoids at 50 % probability, H atoms and the tetrachloridogallate are omitted for clarity). Selected bond distances (Å) angles and torsion angles (°): C1-P1 1.844(2), P1-P2 2.2285(8), P2-N3 1.6790(19), P1-C34 1.854(2), P2-C37 1.873(2), C1-P1-P2 102.76(7), C1-P1-C34 103.59(9), P1-P2-N3 101.88(7), P1-P2-C37 95.38(8)

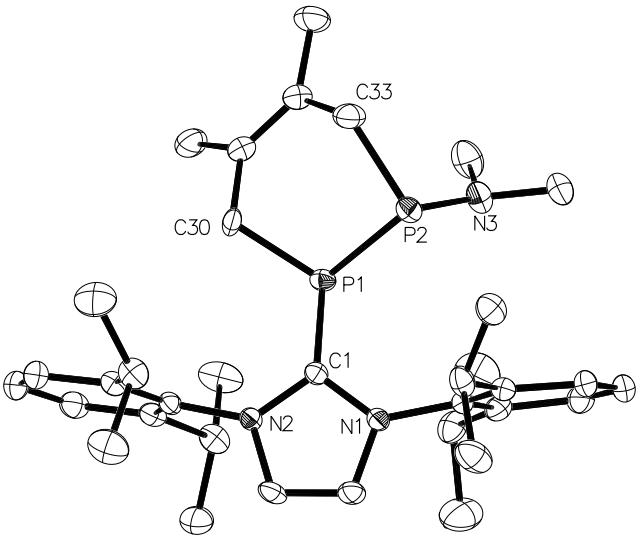

Figure 9 Molecular structure of **4c** (thermal ellipsoids at 50 % probability, H atoms and a disordered tetrachloridogallate are omitted for clarity). Selected bond distances (Å), and angles (°): C1-P1 1.8448(18), P1-P2 2.2204(7), P2-N3 1.6899(18), P1-C30 1.8761(18), P2-C33 1.879(2), C1-P1-P2 103.00(6), C1-P1-C30 106.26(8), P1-P2-N3 99.07(6), P1-P2-C33 95.66(7)

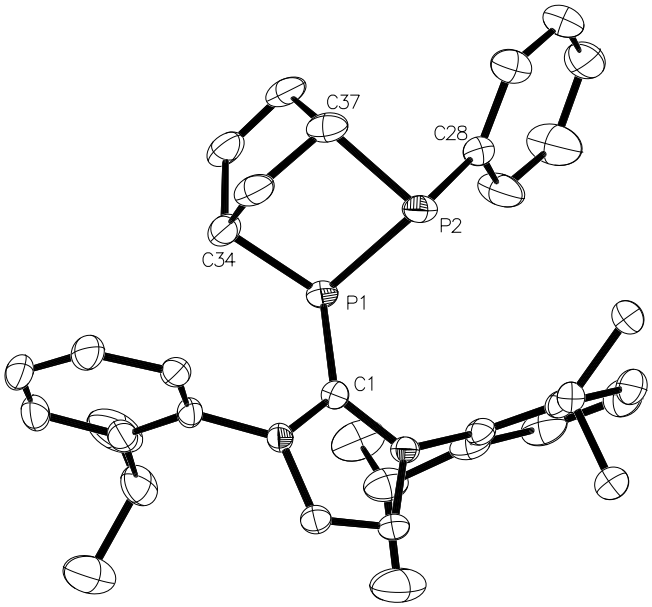

Figure 10 Molecular structure of **5a** (thermal ellipsoids at 50 % probability, H atoms, tetrachloridogallate and the isopropyl moiety at C9 are omitted for clarity. Residual electron density (ca. 3 % of a phosphorus atom) close to P1 and P2 has been assigned to a partial disorder. Due to the low percentage of disorder it was only possible to refine positions for P1A and P2A isotropically). Selected bond distances (Å) and angles (°): C1-P1 1.8501(17), P1-P2 2.2343(6), P2-C28 1.828(2), P1-C34 1.8920(19), P2-C37 1.900(2), C1-P1-P2 96.89(5), C1-P1-C34 106.60(8), P1-P2-C28 103.24(7), P1-P2-C37 89.82(7)

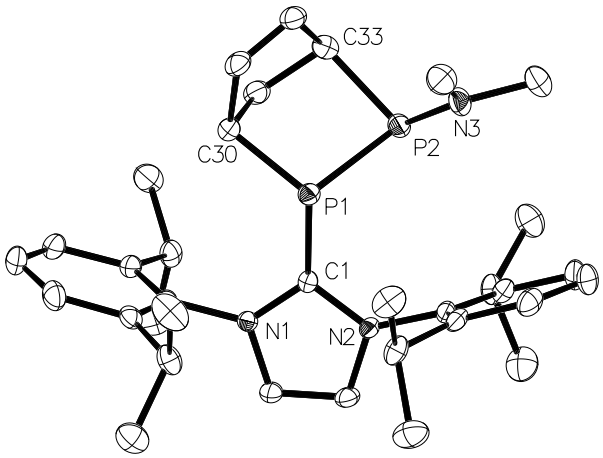

Figure 11 Molecular structure of **5c** (thermal ellipsoids at 50 % probability, H atoms and a disordered tetrachloridogallate are omitted for clarity). Selected bond distances (Å) and angles (°): C1-P1 1.850(3), P1-P2 2.2623(10), P2-N3 1.678(3), P1-C30 1.895(3), P2-C33 1.895(3), C1-P1-P2 99.55(8), C1-P1-C30 107.53(13), P1-P2-N3 102.12(9), P1-P2-C33 88.56(9)

Conclusion

The parent phosphinidene-carbene adduct ^{Dipp}NHC=PH **1** can be coupled with different chlorophosphanes yielding the NHC-supported chlorodiphosphanes **2a-c**. Upon chloride abstraction with the mild Lewis acid $GaCl_3$, cationic derivatives with high P-P double bond character are obtained. Depending on the steric demand and the electronic properties of the substituents R in $[NHC\text{-}P{=}P\text{-}R]^+$, these cations either remain monomeric (**3b**) or dimerise in a [2+2] cycloaddition reaction forming the dicationic cyclotetraphosphanes $\mathbf{(3a)_2}$ and $\mathbf{(3c)_2}$. Amino groups electronically stabilize the $[NHC\text{-}P{=}P\text{-}NR_2]^+$ cations such that even the monomeric dimethylamino derivative can be observed. The monomeric diphosphene cations undergo hetero-DIELS-ALDER reactions with dienes forming cationic NHC-substituted 1,2-diphosphinanes. Given the ease of synthesis and that both the NHC and substituents R at the phosphorus centre can be broadly varied, a new synthesis of functionalized and reactive diphosphenes, $[NHC\text{-}P{=}P\text{-}R]^+$, can be envisioned.

Experimental

Due to the high oxygen and moisture sensitivity of the reported compounds, all reactions mentioned herein have been performed under dry argon using standard Schlenk technique or a glovebox. Solvents and reagents have been degassed and dried prior to use. All reactions have been carried out at ambient temperature. Subsequently, we describe general synthetic procedures for the compounds described herein. An overview of the ^{31}P NMR shifts is given in table 1. Please check the SI for detailed descriptions of the syntheses of the individual compounds including full NMR characterisations and powder diffractograms.

For the preparation of **2a** and **2b**, the dichlorophosphanes, PCl_2Ph and $PCl_2(N^iPr_2)$ respectively, are stirred in a minimum amount of THF or DME and solutions of a small excess of DABCO (1.03 to 1.05 eq.) and one equivalent of NHC=PH **1** in THF or DME are added. A colourless solid (DABCO·HCl) precipitates and the colour changes from pale yellow to deep yellow or green, respectively. After evaporating the reactions mixtures *in vacuo*, **2a** and **2b** are obtained as yellow solids by repeated hexane extraction of the obtained solids. In case of **2a**, the precipitate has been removed by filtration prior to evaporation.

In contrast, for the synthesis of **2c** a solution of NHC=PH **1** in THF is added to a stirred solution of chlorobis(dimethylamino)phosphane (2.2 eq.) and DABCO (1.01 eq.) in THF over 10 min. A colourless solid precipitates and the colour changes from pale to intense yellow.

After stirring the reaction mixture for 2 h, all volatiles are removed *in vacuo*. Repeated hexane extraction of the obtained solid yields **2c** as orange material.

Cationic derivatives **(3a)$_2$**, **3b**, and **(3c)$_2$** are obtained from solutions of **2a-c** in DME or THF by the addition of a small excess of $GaCl_3$ in a minimum amount of hexane. Crystalline **3b** and **(3c)$_2$** have been obtained by layering DME solutions with hexane and diisopropyl ether, respectively.

For the preparation of cycloaddition products **4a-4c** and **5a-5c**, solutions of **2a-c** and large excesses of the diene (1,3-dimethylbuta-1,3-diene or cyclopenta-1,3-diene, respectively) in DME or THF are treated with $GaCl_3$ (1.0-1.05 eq.) in hexane. Compounds **4a-c**, **5a** and **5c** are obtained as crystalline materials via recrystallization of the crude products from DME or DCM and hexane. While **4a-c** and **5a** are stable, **5c** undergoes a cycloreversion reaction when exposed to vacuum yielding both **3c** and **(3c)$_2$**. In case of **5b** and **5b'**, the back reaction is so favourable that the cycloaddition products have only been observed in solution (*cf.* SI for NMR spectra).

Acknowledgements

We thank Dr. Jens Henning, Dr. Michael Wörle and Dr. Nils Trapp for their help with X-ray structure analyses and Mark Bispinghoff for the preparation of ^{Dipp}NHC=PH starting material. A.B. thanks the Studienstiftung des deutschen Volkes and the Dr. Karl Wamsler Stiftung GmbH for scholarships. R.J.G. is grateful to the United Negro College Fund, the Merck Foundation and Merck & Co., Inc. for postdoctoral funding - 2014 UNCF-MERCK Science Research Fellowship.

Notes and References

1. A. J. Arduengo, R. L. Harlow and M. Kline, *Journal of the American Chemical Society*, 1991, **113**, 361-363.
2. A. Igau, H. Grutzmacher, A. Baceiredo and G. Bertrand, *Journal of the American Chemical Society*, 1988, **110**, 6463-6466.
3. D. J. D. Wilson and J. L. Dutton, *Chemistry – A European Journal*, 2013, **19**, 13626-13637.
4. Y. Wang and G. H. Robinson, *Inorganic Chemistry*, 2014, **53**, 11815-11832.
5. C. D. Martin, M. Soleilhavoup and G. Bertrand, *Chemical Science*, 2013, **4**, 3020-3030.
6. M. N. Hopkinson, C. Richter, M. Schedler and F. Glorius, *Nature*, 2014, **510**, 485-496.
7. C. A. Dyker and G. Bertrand, *Science*, 2008, **321**, 1050-1051.
8. D. P. Curran, A. Solovyev, M. Makhlouf Brahmi, L. Fensterbank, M. Malacria and E. Lacôte, *Angewandte Chemie International Edition*, 2011, **50**, 10294-10317.
9. H. Braunschweig, R. D. Dewhurst, K. Hammond, J. Mies, K. Radacki and A. Vargas, *Science*, 2012, **336**, 1420-1422.
10. G. Frenking and N. Holzmann, *Science*, 2012, **336**, 1394-1395.
11. Y. Wang, Y. Xie, P. Wei, R. B. King, H. F. Schaefer, P. von R. Schleyer and G. H. Robinson, *Science*, 2008, **321**, 1069-1071.
12. Y. Wang, Y. Xie, P. Wei, R. B. King, I. I. I. H. F. Schaefer, P. v. R. Schleyer and G. H. Robinson, *Journal of the American Chemical Society*, 2008, **130**, 14970-14971.
13. Y. Wang, Y. Xie, M. Y. Abraham, R. J. Gilliard, P. Wei, H. F. Schaefer, P. v. R. Schleyer and G. H. Robinson, *Organometallics*, 2010, **29**, 4778-4780.
14. J. D. Masuda, W. W. Schoeller, B. Donnadieu and G. Bertrand, *Journal of the American Chemical Society*, 2007, **129**, 14180-14181.
15. O. Back, B. Donnadieu, P. Parameswaran, G. Frenking and G. Bertrand, *Nature Chemistry*, 2010, **2**, 369-373.
16. K. Schwedtmann, M. H. Holthausen, K.-O. Feldmann and J. J. Weigand, *Angewandte Chemie International Edition*, 2013, **52**, 14204-14208.
17. F. D. Henne, E.-M. Schnöckelborg, K.-O. Feldmann, J. Grunenberg, R. Wolf and J. J. Weigand, *Organometallics*, 2013, **32**, 6674-6680.
18. V. D. Romanenko, V. L. Rudzevich, E. B. Rusanov, A. N. Chernega, A. Senio, J.-M. Sotiropoulos, G. Pfister-Guillouzo and M. Sanchez, *Journal of the Chemical Society, Chemical Communications*, 1995, DOI: 10.1039/C39950001383, 1383-1385.
19. A. M. Tondreau, Z. Benko, J. R. Harmer and H. Grützmacher, *Chemical Science*, 2014, **5**, 1545-1554.
20. K. Hansen, T. Szilvási, B. Blom, E. Irran and M. Driess, *Chemistry – A European Journal*, 2014, **20**, 1947-1956.
21. A. Doddi, D. Bockfeld, T. Bannenberg, P. G. Jones and M. Tamm, *Angewandte Chemie International Edition*, 2014, **53**, 13568-13572.
22. M. Bispinghoff, A. M. Tondreau, H. Grutzmacher, C. A. Faradji and P. G. Pringle, *Dalton Transactions*, 2015, DOI: 10.1039/C5DT01741F.
23. L. Liu, D. A. Ruiz, F. Dahcheh and G. Bertrand, *Chemical Communications*, 2015, DOI: 10.1039/C5CC05241F.
24. O. Back, M. Henry-Ellinger, C. D. Martin, D. Martin and G. Bertrand, *Angewandte Chemie International Edition*, 2013, **52**, 2939-2943.
25. CCDC 1415566-1415574 contain the supplementary crystallographic data for this paper. These data can be obtained free of charge from The Cambridge Crystallographic Data Centre via www.ccdc.cam.ac.uk/data_request/cif

26. If bond lengths for comparision are given without further reference to isolated compounds, values are the sums of covalent radii corrected by the influence of the bond polarity as listed by N. Wiberg, in *Lehrbuch der Anorganischen Chemie*, de Gruyter, Berlin, New York, 102nd edn., 2007, p. 2006
27. N. Wiberg, in *Lehrbuch der Anorganischen Chemie*, de Gruyter, Berlin, New York, 102nd edn., 2007, pp. 743-821.
28. N. Wiberg, in *Lehrbuch der Anorganischen Chemie*, de Gruyter, Berlin, New York, 102nd edn., 2007, p. 2006.
29. M.Nieger, E.Niecke, R.Serwas; Private Communication 2002, CCDC 178054
30. A. S. Batsanov, S. M. Cornet, K. B. Dillon, A. E. Goeta, P. Hazendonk and A. L. Thompson, *Journal of the Chemical Society, Dalton Transactions*, 2002, DOI: 10.1039/B207327G, 4622-4628.
31. J. J. Weigand, K.-O. Feldmann and F. D. Henne, *Journal of the American Chemical Society*, 2010, **132**, 16321-16323.
32. M.Nieger, E.Niecke, R.Serwas; Private Communication 2002, CCDC 178054
33. J. J. Daly and L. Maier, *Nature*, 1965, **208**, 383-384.
34. J. Bart, *Acta Crystallographica Section B*, 1969, **25**, 762-770.
35. T. L. Breen and D. W. Stephan, *Organometallics*, 1997, **16**, 365-369.
36. J. J. Daly and L. Maier, *Nature*, 1964, **203**, 1167-1168.
37. J. Bresien, C. Hering, A. Schulz and A. Villinger, *Chemistry – A European Journal*, 2014, **20**, 12607-12615.
38. W. Frank, V. Petry, E. Gerwalin and G. J. Reiss, *Angewandte Chemie International Edition in English*, 1996, **35**, 1512-1514.
39. E. Fluck, R. Riedel, H. D. Hausen and G. Heckmann, *Zeitschrift für anorganische und allgemeine Chemie*, 1987, **551**, 85-94.
40. A. W. N. Wiberg, H.-W. Lerner, K. Karaghiosoff, *Zeitschrift für Naturforschung, B: Chemical Sciences*, 2002, **57**, 1027-1035.
41. N. Burford, C. A. Dyker, M. Lumsden and A. Decken, *Angewandte Chemie International Edition*, 2005, **44**, 6196-6199.
42. S. D. Riegel, N. Burford, M. D. Lumsden and A. Decken, *Chemical Communications*, 2007, DOI: 10.1039/B707741F, 4668-4670.
43. C. A. Dyker, N. Burford, G. Menard, M. D. Lumsden and A. Decken, *Inorganic Chemistry*, 2007, **46**, 4277-4285.
44. J. J. Weigand, N. Burford, R. J. Davidson, T. S. Cameron and P. Seelheim, *Journal of the American Chemical Society*, 2009, **131**, 17943-17953.
45. M. H. Holthausen, D. Knackstedt, N. Burford and J. J. Weigand, *Australian Journal of Chemistry*, 2013, **66**, 1155-1162.
46. L. Heuer, L. Ernst, R. Schmutzler and D. Schomburg, *Angewandte Chemie International Edition in English*, 1989, **28**, 1507-1509.
47. S. J. Geier, M. A. Dureen, E. Y. Ouyang and D. W. Stephan, *Chemistry – A European Journal*, 2010, **16**, 988-993.
48. Y.-y. Carpenter, N. Burford, M. D. Lumsden and R. McDonald, *Inorganic Chemistry*, 2011, **50**, 3342-3353.
49. K.-O. Feldmann and J. J. Weigand, *Angewandte Chemie International Edition*, 2012, **51**, 7545-7549.
50. M. Donath, E. Conrad, P. Jerabek, G. Frenking, R. Fröhlich, N. Burford and J. J. Weigand, *Angewandte Chemie International Edition*, 2012, **51**, 2964-2967.
51. J. Bresien, K. Faust, A. Schulz and A. Villinger, *Angewandte Chemie International Edition*, 2015, **54**, 6926-6930.
52. P. P. Power, *Chemical Reviews*, 1999, **99**, 3463-3504.

53. C. Hering, A. Schulz and A. Villinger, *Angewandte Chemie International Edition*, 2012, **51**, 6241-6245.
54. A. Velian, M. Nava, M. Temprado, Y. Zhou, R. W. Field and C. C. Cummins, *Journal of the American Chemical Society*, 2014, **136**, 13586-13589.
55. When the *exo-endo* nomenclature is used to describe bicyclic cycloaddition products, the term *exo* states that the larger carbene substituent is on the same side of the bicycle as the smaller, i.e. shorter, handle.
56. J. Grobe, A. Armbrecht, D. L. Van, B. Krebs, J. Kuchinke, M. Läge and E. U. Würthwein, *Zeitschrift für anorganische und allgemeine Chemie*, 2001, **627**, 1241-1247.
57. C. Couret, J. Escudie, H. Ranaivonjatovo and J. Satge, *Organometallics*, 1986, **5**, 113-117.
58. G. Fritz, T. Vaahs, W. Hönle and H. G. v. Schnering, *Zeitschrift für anorganische und allgemeine Chemie*, 1987, **552**, 34-49.
59. J. Grobe, D. Le Van and S. Martin, *Zeitschrift für anorganische und allgemeine Chemie*, 1989, **579**, 35-46.

From the Parent Phosphinidene-Carbene Adduct NHC=PH to Cationic P_4-Rings and P_2-Cycloaddition Products

Andreas Beil,[a] *Robert J. Gilliard, Jr.,*[a] *Hansjörg Grützmacher*[a]*

[a] Laboratory of Inorganic Chemistry, ETH Zürich, Vladimir-Prelog-Weg 1, 8093 Zürich, Switzerland.
E-mail: hgruetzmacher@ethz.ch

Supporting Information

Preparations and Experiments 3

1. General Considerations 3

2. Carbene Stabilised Chlorodiphosphanes 4

Synthesis of DippNHC=PPClPh (**2a**) 4

Synthesis of ^{Dipp}NHC=PPCl(N^{i}Pr$_2$) (**2b**) 4

Synthesis of ^{Dipp}NHC=PPCl(NMe$_2$) (**2c**) 6

3. Cationic Derivatives 8

Mass and NMR Data of the Postulated [2+2] Cycloadduct (**3a**)$_2$ 8

Synthesis of ^{Dipp}NHC=PP(N^{i}Pr$_2$)(GaCl$_4$) (**3b**) 9

Synthesis of (^{Dipp}NHC=PPNMe$_2$)$_2$(GaCl$_4$)$_2$ (**3c**)$_2$ 10

Cycloreversion Reaction of **3c**$_2$ upon Heating 11

4. Cycloadducts with 2,3-Dimethylbuta-1,3-diene 12

Synthesis of Cycloadduct **4a** 12

Synthesis of Cycloadduct **4b** 13

Synthesis of Cycloadduct **4c** 15

5. Cycloadducts with Cyclopentadiene 16

Synthesis of Cycloadduct **5a** 16

The Reaction of **3b** with Cyclopentadiene – Proof of Reversibility 18

Synthesis of Cycloadduct **5c** 20

Crystallographic Tables 22

References 32

Preparations and Experiments

1. General Considerations

Starting material ^{Dipp}NHC=PH **1**[1] was synthesised from sodium phosphaethynolate[2, 3] and 1,3-bis(2,6-diisopropylphenyl)-1*H*-imidazol-3-ium chloride[4] according to literature procedures. Dichloro(diisopropylamino)phosphane[5] and chlorobis(dimethylamino)phosphane[6] was synthesised as described in literature. Precursors described herein (**2a-c**) have been applied as obtained from hexane extraction of crude material without further purification. All other reagents and solvents have been purchased from commercial suppliers. 2,3-Dimethylbuta-1,3-diene was distilled from $NaBH_4$ and degassed. Cyclopentadiene was distilled from dicyclopentadiene over copper powder and stored over molecular sieve 3 Å at -30 °C. Solvents have been degassed and purified using an INNOVATIVE TECHNOLOGIES PURE SOLV solvent purification system prior to use. All syntheses and manipulations have been performed in argon under the exclusion of air and moisture using standard SCHLENK technique or a M. BRAUN glovebox.

Single crystal X-ray diffraction measurements were performed on BRUKER SMART APEX, SMART APEX2 or D8 VENTURE systems. Data analysis were performed using BRUKER APEX2 and OLEX2 1.2 software.[7] CCDC numbers (1415566-1415574) are listed in the crystallographic tables. Powder diffraction measurements were performed on a STOE system. From single crystal data, powder patterns have been calculated using MERCURY 3.3 and plotted together with the measured data using ORIGIN PRO 9.1 in order to prove the identity of the bulk product. Due to the extreme sensitivity of these compounds to oxidation, we were only able to obtain analytical pure material of **2a**.

NMR spectra have been recorded on BRUKER 250, 300, 400 and 500 MHz spectrometers. Deuterated solvents have been degassed and dried prior to use. Chemical shifts are reported in ppm relative to $SiMe_4$ (for ^{1}H and ^{13}C) and 85 % phosphoric acid (for ^{31}P) using the solvent deuterium signals as internal standards. Signal multiplicities are described as singlet (s), doublet (d), triplet (t), quartet (q), septet (sept), multiplet (m) and broad singlet (bs). For ^{13}C signals overlapping with solvent residual signals, shifts have been taken from DEPT 135 spectra. Data analysis has been carried out using BRUKER TOPSPIN 3.1.

MALDI-TOF mass spectra were recorded at the ETH Zürich MS department on a BRUKER ULTRAFLEX II system. Elemental analyses have been carried out at the ETH Zürich Mikrolabor.

2. Carbene Stabilised Chlorodiphosphanes

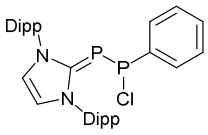

2a

Synthesis of DippNHC=PPClPh (**2a**)

Dichlorophenylphosphane (63.8 mg, 0.36 mmol, 1 eq.) is dissolved in 0.2 mL of dry THF. A solution of **1** (149.7 mg, 0.36 mmol, 1 eq.) in 2 mL of dry THF and DABCO (41.3 mg, 0.37 mmol, 1.03 eq.) in 1 mL of dry THF are added. The colour changes from pale to deep yellow and a colourless solid precipitates immediately. The reaction mixture is filtered over a PTFE syringe filter and evaporated *in vacuo*. The obtained orange foam is extracted 6 × with 10 mL of hexane. Evaporation of the combined yellow hexane fractions yields ^{Dipp}NHC=PPClPh (**2a**) as yellow solid (74.3 mg, 0.13 mmol, 36 %). Single crystals suitable for X-ray crystallography have been obtained by slow evaporation of a hexane solution of **2a**. A minimum amount of analytically pure material has been obtained from hexane at -30 °C.

^{1}H NMR (500 MHz, THF-d$_8$, 298 K) δ = 7.48 (t, J_{HH} = 7.8 Hz, 2H, p-Dipp), 7.45-7.40 (m, 2H, Ph), 7.38 (s, 2H, C*H*=C*H*), 7.33 (m, 4H, m-Dipp), 7.09 (t J_{HH} = 7.5 Hz, 2H, Ph), 7.07-7.02 (m, 1H, Ph), 2.93 (sept., J_{HH} = 7.0 Hz, 2H, Dipp-C*H*(CH$_3$)$_2$), 2.85 (sept., J_{HH} = 6.9 Hz, 2H, Dipp-C*H*(CH$_3$)$_2$), 1.41 (d, J_{HH} = 6.9 Hz, 12H, Dipp-C*H*$_3$), 1.23 (d, J_{HH} = 6.9 Hz, 12H, Dipp-C*H*$_3$); **^{13}C{^{1}H} NMR** (125.8 MHz, THF-d$_8$, 298 K) δ = 169.9 (dd, J_{PC} = 119.0 Hz, J_{PC} = 20.8 Hz, C$_{carbene}$), 146.18 (d, J = 33.9 Hz, ipso-Dipp), 124.0 (m-Dipp), 123.1 (d, J_{PC} = 3.6 Hz, *C*H=*C*H), 29.0 (Dipp-*C*H(CH$_3$)$_2$), 28.9 (Dipp-*C*H(CH$_3$)$_2$), 24.2 (*C*H$_3$), 24.1 (*C*H$_3$), 22.4 (*C*H$_3$), 22.2 (*C*H$_3$); **^{31}P{^{1}H} NMR** (202.5 MHz, THF-d$_8$, 298 K) δ = 157.6 (d, J_{PP} = 374.5 Hz), -17.3 (d, J_{PP} = 377.9 Hz); **EA** calc. for $C_{33}H_{41}N_2P_2Cl$: C 70.39, H 7.34, N 4.97, found: C 70.67, H 7.57, N 4.95

Synthesis of ^{Dipp}NHC=PPCl(N^{i}Pr$_2$) (**2b**)

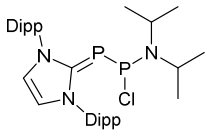

2b

Dichloro(diisopropylamino)phosphane (130.6 mg, 0.646 mmol, 1 eq.) is dissolved in 0.5 mL of THF and a solution of DABCO (76 mg, 0.68 mmol, 1.05 eq.) in a minimum amount of THF is added. Upon addition of this solution to a pale yellow solution of ^{Dipp}NHC=PH (271.7 mg, 0.646 mmol, 1 eq.) in a minimum amount of THF, the colour changes to bright green and a colourless solid precipitates immediately. The crude reaction mixture is evaporated *in vacuo*, ca. 50 mL of dry

hexane are added and the mixture is sonicated for 10 min yielding a greenish suspension. Filtration over a PTFE syringe filter results in a bright yellow solution, which is evaporated *in vacuo* yielding ^{Dipp}NHC=PPCl(N^{i}Pr$_2$) (**2b**) as yellow solid (323 mg, 0.551 mmol, 85 %). Single crystals suitable for X-ray crystallography have been obtained by slow evaporation of a hexane solution of **2b**.

^{1}H NMR (400 MHz, C_6D_6, 298 K) δ = 7.24 (m, 2H, p-*Ar*), 7.13 (d, J_{HH} = 7.8 Hz, 4H, m-*Ar*), 6.28 (s, 2H, C*H*=C*H*), 3.02 (sept., J_{HH} = 6.8 Hz, 4H, Dipp-C*H*(CH$_3$)$_2$), 1.55 (d, J_{HH} = 6.8 Hz, 12H, Dipp- CHC^a*H*$_3$C^{b}H$_3$), 1.34—1.19 (m, 2H, NC*H*(CH$_3$)$_2$), 1.10 (d, J_{HH} = 6.9 Hz, 12H, Dipp-CHC^{a}H$_3$C^b*H*$_3$), 1.06—0.92 (m, 12H, NCH(C*H*$_3$)$_2$); **^{13}C{^{1}H} NMR** (100.6 MHz, C_6D_6, 298 K) δ = 171.6 (dd, J_{PC} = 110.4 Hz, J_{PC} = 31.3 Hz, $C_{carbene}$), 146.6 (o-Dipp), 134.5 (d, J = 1.8 Hz, ipso-Dipp), 130.3 (p-Dipp), 124.5 (m-Dipp), 121.6 (d, J_{PC} = 3.2 Hz, *C*H=*C*H), 28.9 (Dipp-*C*H(CH$_3$)$_2$), 24.7 (Dipp-CHC^{a}H$_3$*C*^{b}H$_3$), 23.2 (Dipp-CH*C*^{a}H$_3$C^{b}H$_3$), 22.7 (NCH(*C*H$_3$)$_2$), not found: (N*C*H(CH$_3$)$_2$); **^{31}P{^{1}H} NMR** (162.0 MHz, C_6D_6, 298 K) δ = 213.0 (d, J_{PP} = 337.0 Hz), -16.7 (d, J_{PP} = 336.1 Hz); **^{31}P{^{1}H} NMR** (202.5 MHz, THF-d$_8$, 298 K) δ = 215.1 (d, J_{PP} = 342.2 Hz), -18.4 (d, J_{PP} = 342.1 Hz)

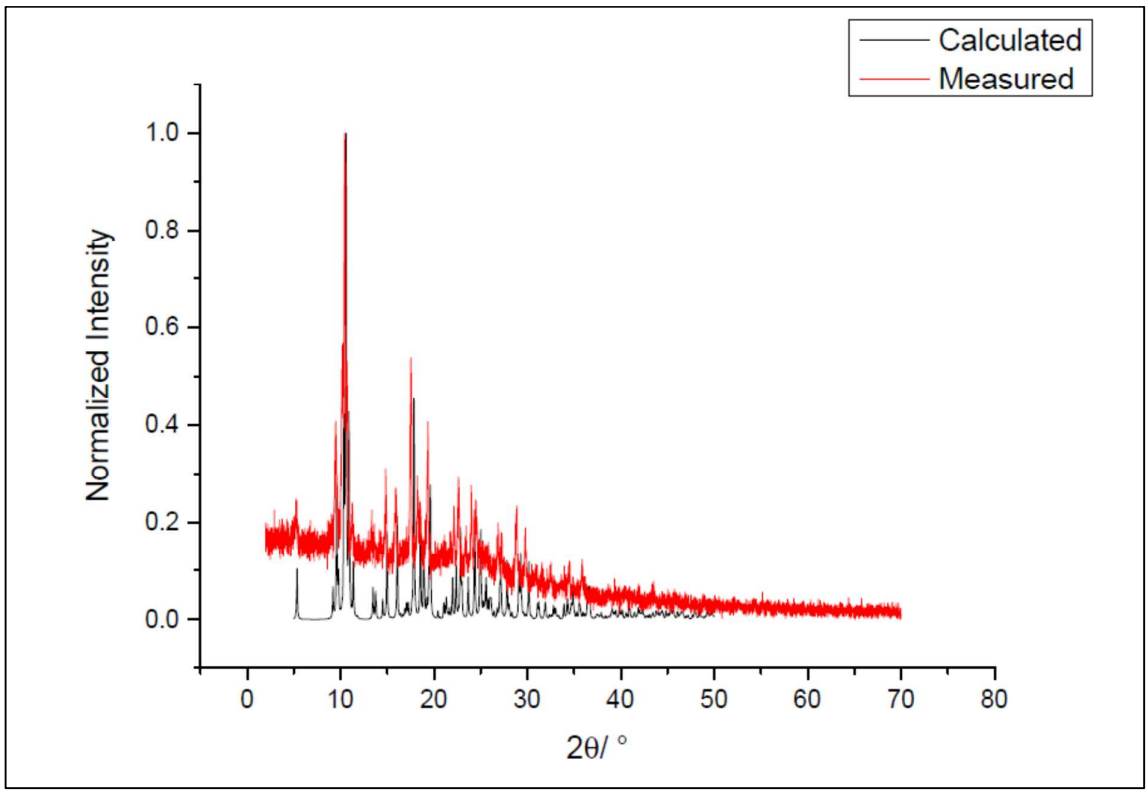

Figure S 1 Calculated and measured powder diffractograms of **2b**

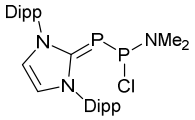

2c

Synthesis of ^{Dipp}NHC=PPCl(NMe$_2$) (**2c**)

Chlorobis(dimethylamino)phosphane (257.6 mg, 1.67 mmol, 2.2 eq.) is dissolved in 2 mL of THF and a solution of DABCO (86.6 mg, 0.772 mmol, 1.01 eq.) in 2 mL of THF is added. While stirring at r.t., a solution of **1** (320.0 mg, 0.761 mmol, 1.0 eq.) in 10 mL of THF is added dropwise over 10 min. The solution turns from pale to intense yellow and a solid precipitates. After stirring the reaction mixture for 2 h at r.t., the solvent is removed *in vacuo*. An olive green mass is obtained, which is treated with dry hexane (2 × 100 mL) upon sonication. The yellow hexane solution is filtered off. Evaporation *in vacuo* gives **2c** as dirty orange crystalline solid (278.2 mg, 0.525 mmol, 69 %), which is used for further conversions.

We were not able to obtain a publishable structure of **2c**. However, for the calculation of a powder pattern a low quality molecular structure (data not shown) of **2c** has been used. The measured powder pattern shows good accordance with the calculated (Figure S 2).

^{1}H NMR (400 MHz, THF-d$_8$, 298 K) δ = 7.47 (t, J_{HH} = 7.8 Hz, 2H, p-Dipp), 7.31 (d, J_{HH} = 7.8 Hz, 4H, m-Dipp), 7.18 (s, 2H, C*H*=C*H*), 2.89 (sept., J_{HH} = 6.9 Hz, 4H, Dipp-C*H*(CH$_3$)$_2$), 2.39 (d, J_{PH} = 13.5 Hz, 6H, PN(C*H*$_3$)$_2$), 1.39 (d, J_{HH} = 6.8 Hz, 12H, Dipp-C*H*$_3$), 1.21 (d, J_{HH} = 6.9 Hz, 12H, Dipp-C'*H*$_3$); **^{13}C{^{1}H} NMR** (100.6 MHz, THF-d$_8$, 298 K) δ = 170.7 (dd, , J_{PC} = 113.7 Hz, J_{PC} = 24.6 Hz, C$_{carbene}$), 147.1-146.2 (m, ipso-Dipp), 130.0 (p-Dipp), 134.2 (d, *J* = 3.3 Hz, o-Dipp), 124.1 (m-Dipp), 121.9 (d, J_{PC} = 3.5 Hz, *C*H=*C*H), 40.3-39.7 (m, PN(*C*H$_3$)$_2$), 28.8 (Dipp-*C*H(CH$_3$)$_2$), 24.0 (Dipp-CH*C'*H$_3$CH$_3$), 22.2 (Dipp-CHC'H$_3$*C*H$_3$); **^{31}P{^{1}H} NMR** (162.0 MHz, THF-d$_8$, 298 K) δ = 214.1 (d, J_{PP} = 349.2 Hz), -33.5 (d, J_{PP} = 351.0 Hz); **^{31}P NMR** (162.0 MHz, THF-d$_8$, 298 K) δ = 215.6-212.8 (m), -33.6 (d, J_{PP} = 346.8 Hz)

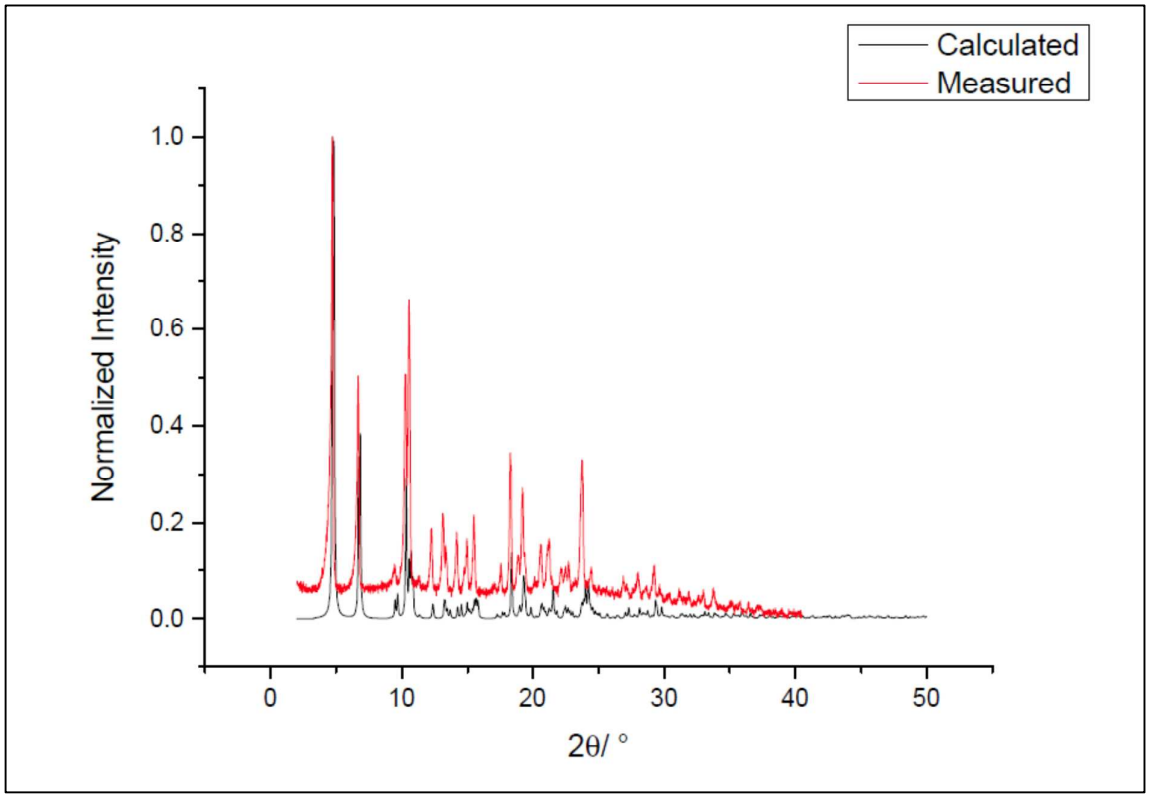

Figure S 2 Calculated and measured powder diffractograms of **2c**

3. Cationic Derivatives

Mass and NMR Data of the Postulated [2+2] Cycloadduct (**3a**)$_2$

^{Dipp}NHC=PPClPh (**2a**) (14.7 mg, 0.026 mmol) and $GaCl_3$ (5.3 mg, 0.030 mmol, 1.15 eq.) are dissolved in 0.5 mL of purified THF-d_8. A clear orange solution is obtained from which NMR spectra are recorded at a BRUKER 400 MHz spectrometer (**Figure S 3**). **^{31}P NMR** (162.0 MHz, THF-d_8, 298 K) δ = -24.2 (t, J_{PP} = 111.9 Hz), -69.3 (t, J_{PP} = 112.1 Hz). A small triplet with J = 107.3 Hz and δ = -66.0 ppm might be assigned to a stereoisomer of the described four membered ring **(3a)$_2$** (of which the corresponding coupling triplet might be located under the strong triplet at δ = -24.2 ppm), while signals around 48 and -126 ppm remain unassigned. MALDI-TOF data of a sample prepared similarly are depicted in **Figure S 4**. The postulation of this structure is also supported by the NMR data of **(3c)$_2$** (δ = 16.6 (t, J_{PP} = 163.3 Hz), -6.9 (t, J_{PP} = 162.9 Hz)), of which the structure is proven by single crystal X-ray diffraction (*vide infra*).

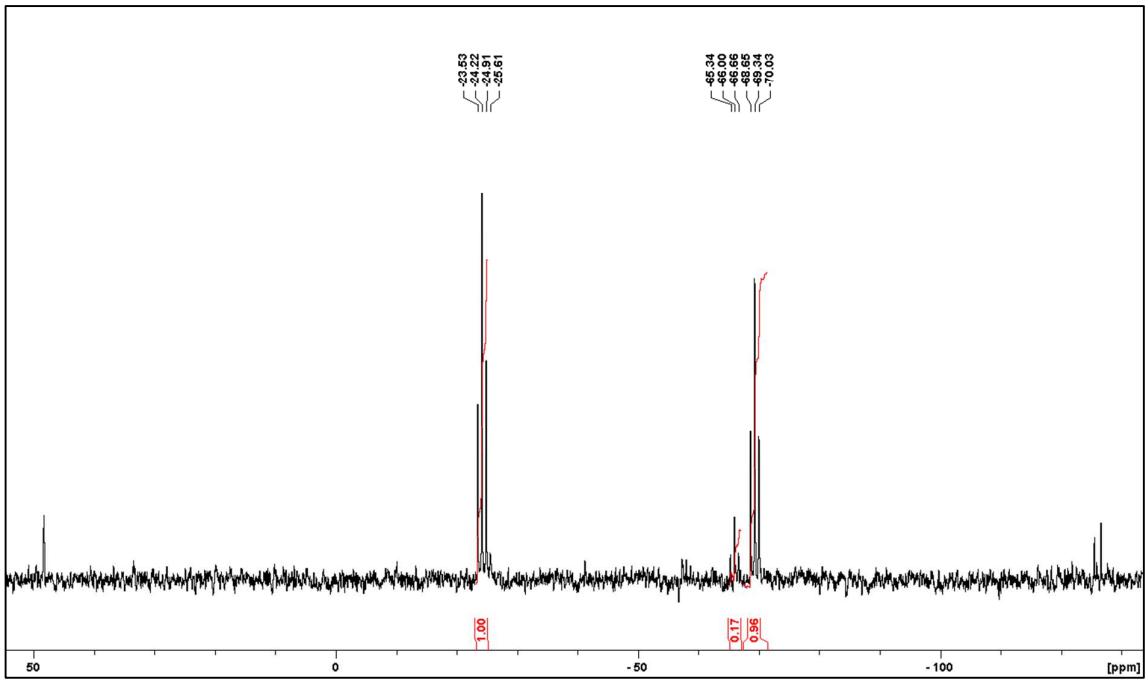

Figure S 3 ^{31}P NMR spectrum of the postulated species **(3a)$_2$**

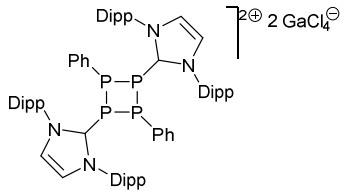

(3a)2

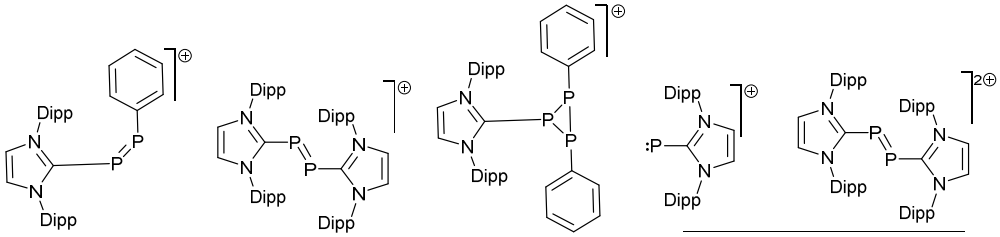

100 %	46.6 %	41.5 %	3.4 %
$C_{33}H_{41}N_2P_2^+$	$C_{54}H_{72}N_4P_2^+$	$C_{39}H_{46}N_2P_3^+$	$C_{27}H_{36}N_2P^+$ or $C_{54}H_{72}N_4P_2^{2+}$
m/z calc. = 527.2745	m/z calc. = 838.5232	m/z calc. = 635.2874	m/z calc. = 419.2616
m/z found = 527.2738	m/z found = 838.5227	m/z found = 635.2869	m/z found = 419.2611

Figure S 4 MALDI-TOF (positive mode) data of a sample prepared similarly to the method described above and assignment of the main signals

Synthesis of ^{Dipp}NHC=PP(N^{i}Pr$_2$)(GaCl$_4$) (**3b**)

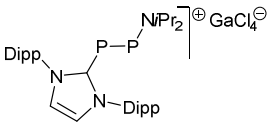

3b

Dipp$_2$NHC=PPCl(N^{i}Pr$_2$) (38.3 mg, 0.07 mmol, 1 eq.) is dissolved in 1 mL of dry DME. Anhydrous GaCl$_3$ (12.3 mg, 0.07 mmol, 1 eq.) in a minimum amount of hexane is added yielding a deep yellow solution. By layering this solution with hexane, crystals suitable for single crystal X-ray crystallography have been obtained which have also been used for NMR spectroscopy. Yield has not been determined.

^{1}H NMR (500 MHz, THF-d$_8$, 298 K) δ = 8.31 (s, 2H, C*H*=C*H*), 7.68 (t, J_{HH} = 7.8 Hz, 2H, p-*Ar*), 7.52 (d, J_{HH} = 7.9 Hz, 4H, m-*Ar*), 4.70 – 3.76 (m, 2H, NC*H*(CH$_3$)$_2$), 2.56 (sept., J_{HH} = 6.8 Hz, 4H, Dipp-C*H*(CH$_3$)$_2$), 1.34 (d, J_{HH} = 6.9 Hz, 12H, Dipp-C*H*$_3$), 1.30 (d, J_{HH} = 6.9 Hz, 12H, Dipp-C*H'*$_3$), 1.16 (d, J_{HH} = 6.6 Hz, 12H, NCH(C*H*$_3$)$_2$); **^{13}C{^{1}H} NMR** (125.8 MHz, THF-d$_8$, 298 K) δ = 145.4 (ipso-Ar), 132.2 (p-Ar), 131.8 (o-Ar), 128.1 (*C*H=*C*H), 125.1 (m-Ar), 29.4 (Dipp-*C*H(CH$_3$)$_2$), 25.9 (NCH(C*H*$_3$)CH'$_3$, only in HSQC), 24.3 (Dipp-CH$_3$), 22.0 (Dipp-CH'$_3$), 19.0 (NCH(CH$_3$)C*H'*$_3$, only in HSCQ), not found: ($C_{carbene}$, N*C*H(CH$_3$)$_2$); **^{31}P{^{1}H} NMR** (202.5 MHz, THF-d$_8$, 298 K) δ = 492.1 (d, J_{PP} = 527.2 Hz), 158.1 (d, J_{PP} = 523.7 Hz)

Synthesis of (^{Dipp}NHC=PPNMe$_2$)$_2$(GaCl$_4$)$_2$ **(3c)$_2$**

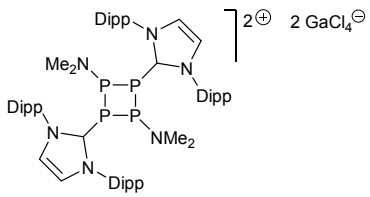

(3c)$_2$

To the yellow solution of **2c** (40.9 mg, 0.077 mmol) in 1 mL of dry THF, a solution of $GaCl_3$ (13.7 mg, 0.077 mmol, 1 eq.) in 0.7 mL of dry hexane is added. Upon evaporating the obtained milky reaction mixture *in vacuo*, a green foam is obtained, which is dissolved in 0.5 mL of dry DME. Covering this solution with dry diisopropyl ether gives **(3c)$_2$** as large colourless crystals (38.5 mg, 0.027 mmol, 70 %) suitable for X-ray diffraction.

^{1}H NMR (500 MHz, THF-d$_8$, 298 K) δ = 8.18 (s, 4H, C*H*=C*H*), 7.75 (t, J_{HH} = 7.8 Hz, 4H, p-Dipp), 7.59 (d, J_{HH} = 7.9 Hz, 8H, m-Dipp), 2.51 (sept., J_{HH} = 7.1 Hz, 8H, Dipp-C*H*(CH$_3$)$_2$), 2.30-1.60 (m, 12H, N(C*H*$_3$)$_2$), 1.44 (d, J_{HH} = 6.9 Hz, 24H, Dipp-C*H*$_3$), 1.24 (d, J_{HH} = 6.8 Hz, 24H, Dipp-C'*H*$_3$), **^{13}C{^{1}H} NMR** (125.8 MHz, THF-d$_8$, 298 K) δ = 145.0 (ipso-Dipp), 133.2 (p-Dipp), 130.6 (o-Dipp), 129.9 (*C*H=*C*H), 126.2 (m-Dipp), 29.7 (Dipp-*C*H(CH$_3$)$_2$), 24.7 (Dipp-CH(*C*H$_3$)$_2$), 22.1 (Dipp-CH(*C*H$_3$)$_2$), not found: N(*C*H$_3$)$_2$, C$_{carbene}$; **^{31}P{^{1}H} NMR** (202.5 MHz, THF-d$_8$, 298 K) δ = 16.6 (t, J_{PP} = 163.3 Hz), -6.9 (t, J_{PP} = 162.9 Hz)

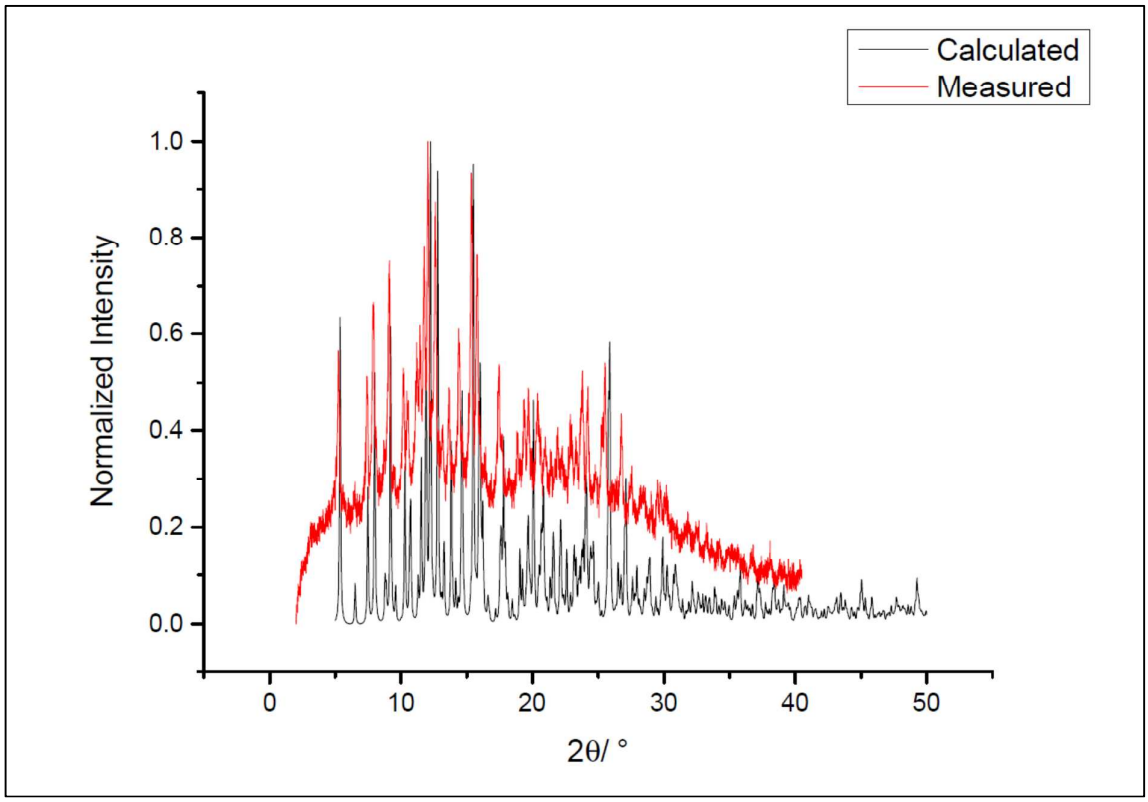

Figure S 5 Calculated and measured powder diffractograms of **(3c)$_2$**

Cycloreversion Reaction of **3c$_2$** upon Heating

The 121.5 MHz ^{31}P NMR spectrum of a solution of **(3c)$_2$** (7.0 mg, 0.005 mmol) and 2,3-dimethylbuta-1,3-diene (45 mg, 0.55 mmol, 220 eq. relative to the monomer) in 0.45 mL of THF in a J. YOUNG type NMR tube equipped with a sealed glass capillary containing 0.85 % D_3PO_4 in D_2O as external NMR standard is recorded. This spectrum (Figure S 6a) shows the signals reported for **(3c)$_2$** (17.0 ppm, t, J = 165.5 Hz and -6.7 ppm, t, J = 164.5 Hz). Subsequently, the sample is heated to 60 °C for 20 h. The spectrum recorded afterwards (Figure S 6b) shows the NMR signals of the cycloadduct **4c** (65.5 ppm, d, J = 228.0 Hz and -41.8 ppm, d, J = 229.4 Hz, *vide infra*) indicating the full conversion of **(3c)$_2$** to **4c**. This proves that **(3c)$_2$** exists monomeric at elevated temperature.

All 121.5 MHz ^{31}P NMR spectra are recorded with 30 s relaxation delay and apodization is applied (a = 10 Hz).

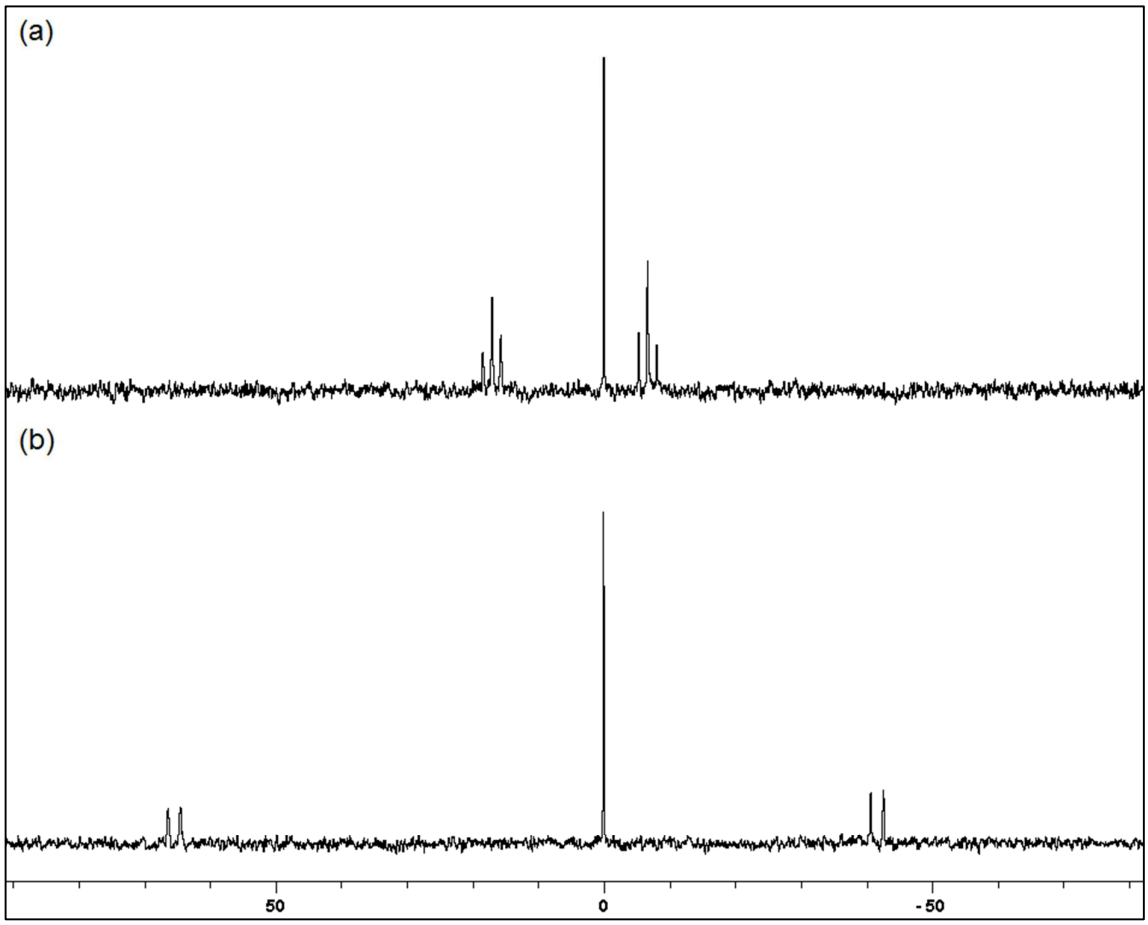

Figure S 6 ^{31}P NMR spectra showing the conversion of **(3c)$_2$** into **4c** upon heating to 60 °C in the presence of 2,3-dimethylbuta-1,3-diene. The signal at 0 ppm is 0.85 % D_3PO_4 in D_2O as external NMR standard

4. Cycloadducts with 2,3-Dimethylbuta-1,3-diene

Synthesis of Cycloadduct **4a**

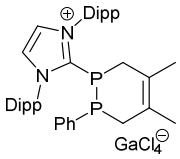

4a

To the deep yellow solution of **2a** (51.6 mg, 0.092 mmol) and 2,3-dimethylbuta-1,3-diene (0.2 mL, ca. 2.4 mmol, ca. 26 eq.) in 3 mL of dry THF, $GaCl_3$ (17.4 mg, 0.099 mmol, 1.08 eq.) in 1 mL of dry hexane is added dropwise while stirring at r.t. After 30 min, the reaction mixture is evaporated *in vacuo* yielding an off-white foam, which is recrystallized twice from a DME solution layered with hexane. **4a** is isolated as off-white crystals suitable for X-ray crystallography (34.7 mg, 0.042 mmol, 46 %).

It is necessary to abstract the Cl atom in presence of the trapping agent as otherwise the *in situ* formed cation dimerises and therefore would not be accessible for a cycloaddition reaction with DMB.

^{1}H NMR (500 MHz, $CDCl_3$, 298 K) δ = 7.84 (s, 2H, C*H*=C*H*), 7.47 (t, J_{HH} = 7.9 Hz, 2H, p-Dipp), 7.30-7.23 (m, 1H, Ph), 7.29 (dd, J_{HH} = 7.8 Hz, J_{HH} = 1.1 Hz, 2H, m-Dipp), 7.25 (dd, J_{HH} = 7.8 Hz, J_{HH} = 1.2 Hz, 2H, m'-Dipp), 7.16-7.11 (m, 2H, Ph), 6.99-6.93 (m, 2H, Ph), 2.58 (sept., J_{HH} = 7.0 Hz, 2H, Dipp-C*H*$(CH_3)_2$), 2.51 (sept., J_{HH} = 7.1 Hz, 2H, Dipp-C*H*$(CH_3)_2$), 2.24 (dt, J_{HH} = 14.4 Hz, J_{HH} = 6.7 Hz, 1H, C'*H*H), 2.03-1.92 (m, 2H, C'*H*H, CH*H*), 1.82 (td, J_{HH} = 11.9 Hz, J_{HH} = 3.5 Hz, 1H, CH*H*), 1.62 (bs, 3H, CH_3), 1.37 (d, J_{HH} = 6.8 Hz, 6H, Dipp-CH_3), 1.37 (d, J_{HH} = 6.8 Hz, 6H, Dipp-CH_3), 1.28 (d, J_{HH} = 6.8 Hz, 6H, Dipp-CH_3), 1.22 (d, J_{HH} = 6.8 Hz, 6H, Dipp-CH_3), 1.19 (d, 3H, J_{PH} = 6.75 Hz, CH_3); **^{13}C{^{1}H} NMR** (125.8 MHz, $CDCl_3$, 298 K) δ = 151.6 (dd, J_{PC} = 81.8 Hz, J_{PC} = 28.2 Hz, $C_{carbene}$), 145.7 (ipso-Dipp), 145.1 (ipso-Dipp), 134.3 (dd, J_{PC} = 262 Hz, J_{PC} = 16 Hz, ipso-Ph), 132.8-132.5 (several signals, p-Dipp, Ph), 130.6 (o-Dipp), 129.3 (Ph), 128.6 (*C*H=*C*H), 128.0 (d, J_{PH} = 6.2 Hz, Ph), 125.0 (m-Dipp), 124.9 (m-Dipp), 33.0 (dd, , J_{PC} = 29.6 Hz, J_{PC} = 3.8 Hz, *C*'HH), 29.7-29.5 (several signals, Dipp-*C*H$(CH_3)_2$), 26.2 (Dipp-CH(*C*$H_3)_2$), 25.7 (Dipp-CH(*C*$H_3)_2$), 24.1 (d, J_{PC} = 25.8 Hz, *C*HH), 22.4-22.2 (several signals, Dipp-CH(*C*$H_3)_2$), 21.6 (d, J_{PC} = 3.5 Hz, *C*H_3), 18.5 (*C*H_3); **^{31}P{^{1}H} NMR** (202.5 MHz, $CDCl_3$,, 298 K) δ = -19.4 (d, J_{PP} = 211.4 Hz), -44.7 (d, J_{PP} = 211.7 Hz)

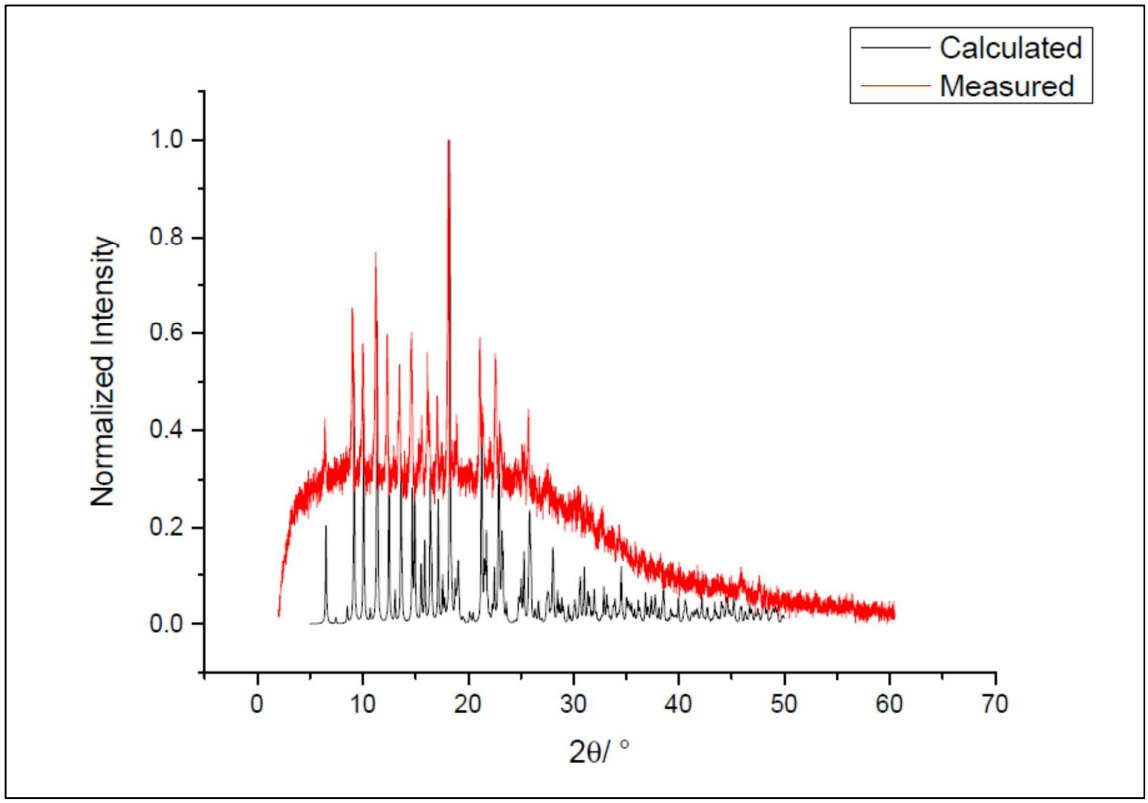

Figure S 7 Calculated and measured powder diffractograms of **4a**

Synthesis of Cycloadduct **4b**

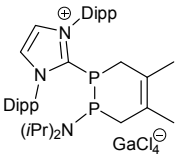

4b

To the deep yellow solution of **2b** (196.7 mg, 0.336 mmol) and 2,3-dimethylbuta-1,3-diene (0.4 mL, ca. 10 eq.) in 4 mL of dry THF, $GaCl_3$ (59.2 mg, 0.336 mmol, 1.0 eq.) in a minimum amount of dry hexane is added while stirring. After concentrating the reaction mixture to one half, 10 mL of dry hexane are added yielding the precipitation of a solid and the formation of an oil. Subsequent evaporation of the whole batch *in vacuo* yields **4b** as a yellow solid (242.8 mg, 0.288 mmol, 86 %). Single crystals suitable for X-ray crystallography have been obtained from a solution of **4b** in DME layered with hexane at r.t.

^{1}H NMR (500 MHz, $CDCl_3$, 298 K) δ = 7.90 (s, 2H, C*H*=C*H*), 7.63 (t, J_{HH} = 7.8 Hz, 2H, p-Dipp), 7.45 (dd, J_{HH} = 7.8 Hz, J_{HH} = 1.1 Hz, 2H, m-Dipp), 7.37 (dd, J_{HH} = 7.8 Hz, J_{HH} = 1.1 Hz, 2H, m'-Dipp), 3.06 (d sept., J_{PH} = 11.8 Hz, J_{HH} = 6.4 Hz, 2H, N(C*H*$(CH_3)_2)_2$), 2.57 (sept., J_{HH} = 6.7 Hz, 2H, Dipp-C*H*$(CH_3)_2$), 2.36 (sept., J_{HH} = 7.1 Hz, 2H, Dipp-C*H*$(CH_3)_2$), 2.30-2.22 (m, 2H, CH*H,* C*H*H), 2.00 (ddd, *J* = 14.8 Hz, *J* = 6.0 Hz, *J* = 3.0 Hz, 1H, C'H*H*), 1.73 (d, 3H, J_{PH} = 5.0 Hz, CH_3), 1.69 (bs, 3H, CH_3), 1.54 (d, J_{HH} = 6.8 Hz, 6H, Dipp-CH_3), 1.32 (d, J_{HH} =

6.8 Hz, 6H, Dipp-CH_3), 1.25 (d, J_{HH} = 6.5 Hz, 6H, Dipp-CH_3), 1.24 (d, J_{HH} = 6.6 Hz, 6H, Dipp-CH_3), 1.02 (d, J_{HH} = 6.6 Hz, 6H, N(CH(CH_3CH$_3$))$_2$), 0.95-0.87 (m, 1H, C'*H*H), 0.83 (d, J_{HH} = 6.6 Hz, 6H, N(CH(CH$_3$CH_3))$_2$), some shifts and coupling constants from 300 MHz and 400 MHz spectra; **^{13}C{^{1}H} NMR** (125.8 MHz, CDCl$_3$, 298 K) δ = 150.9 (dd, , J_{PC} = 85.1 Hz, J_{PC} = 31.4 Hz, $C_{carbene}$), 145.7 (ipso-Dipp), 145.2 (ipso-Dipp), 133.1 (d, J_{PC} = 11.2 Hz, *C*CH$_3$=CH$_3$C), 132.4 (p-Dipp), 131.6 (o-Dipp), 129.4 (d, *C*H=*C*H), 124.9 (m-Dipp), 124.6 (m'-Dipp), 121.1 (d, J_{PC} = 4.1 Hz, CCH$_3$=*C*CH$_3$), 49.8-48.9 (m, N(*C*H(CH$_3$CH$_3$))$_2$), 39.1 (d, J_{PC} = 37.1 Hz, *C*'HH), 27.9 (d, J_{PC} = 21.4 Hz, *C*HH), 30.0-29.5 (several signals, Dipp-*C*H(CH$_3$)$_2$), 26.4 (Dipp-*C*H$_3$), 26.2 (Dipp-*C*H$_3$), 24.3 (d, J_{PC} = 4.4 Hz, N(CH(*C*H$_3$CH$_3$))$_2$), 22.8 (d, J_{PC} = 8.0 Hz, N(CH(CH$_3$*C*H$_3$))$_2$), 22.7-22.3 (several signals, Dipp-CH(*C*H$_3$)$_2$), 21.7 (d, J_{PC} = 2.5 Hz, *C*H$_3$), 19.5 (d, J_{PC} = 16.3 Hz, *C*H$_3$); **^{31}P{^{1}H} NMR** (202.5 MHz, CDCl$_3$,, 298 K) δ = 32.9 (d, J_{PP} = 239.9 Hz), -56.5 (d, J_{PP} = 238.7 Hz); impurities observed in NMR

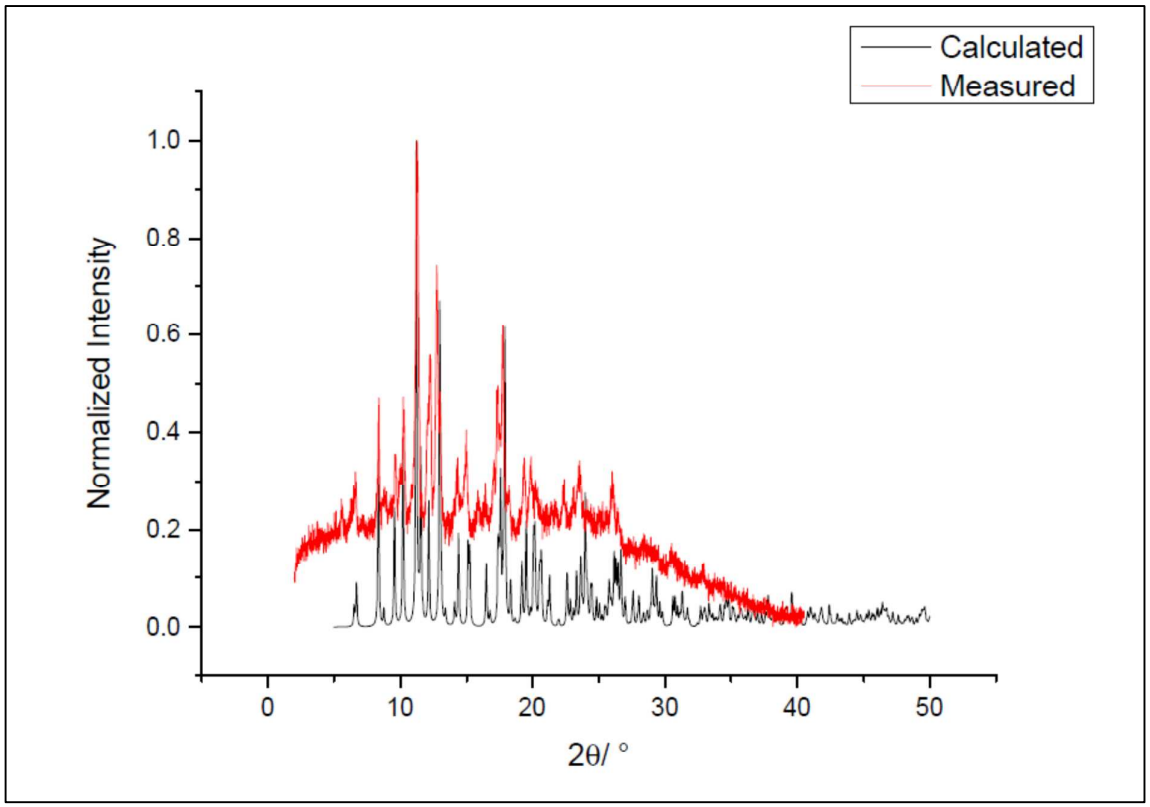

Figure S 8 Calculated and measured powder diffractograms of **4b**

Synthesis of Cycloadduct **4c**

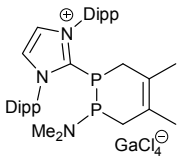

4c

To a stirred solution of **2c** (86.4 mg, 0.163 mmol) and 2,3-dimethylbuta-1,3-diene (0.1 mL, ca. 0.9 mmol, ca. 5.5 eq.) in 3 mL of DME, a solution of $GaCl_3$ (29.2 mg, 0.166 mmol, 1.02 eq.) in 1.5 mL of hexane is added dropwise. After stirring for 30 min at r.t., the reaction mixture is evaporated *in vacuo*. The residue is dissolved in 5 mL of DME, filtered over a PTFE syringe filter, covered with 5 mL of hexane and left for crystallisation. **4c** is obtained as pale green crystals suitable for X-ray diffraction (52.5 mg, 0.067 mmol, 41 %).

^{1}H NMR (400 MHz, $CDCl_3$, 298 K) δ = 7.76 (s, 2H, C*H*=C*H*), 7.64 (t, J_{HH} = 7.8 Hz, 2H, p-Dipp), 7.41 (d, J_{HH} = 7.8 Hz, 2H, m-Dipp), 7.38 (d, J_{HH} = 7.8 Hz, 2H, m'-Dipp), 2.56 (sept., J_{HH} = 6.9 Hz, 2H, Dipp-C*H*$(CH_3)_2$), 2.48 (sept., J_{HH} = 7.0 Hz, 2H, Dipp-C*H*$(CH_3)_2$), 2.29 (ddd, J_{HH} = 14.9 Hz, J_{HH} = 6.8 Hz, J_{HH} = 2.5 Hz, 1H, C*H*H), 2.16 (d, J_{PH} = 9.6 Hz, 6H, N(CH_3)$_2$), 2.02-1.91 (m, 1H, C'*H*H), 1.72 (d, J_{PH} = 6.3Hz, 3H, CH_3), 1.70-1.61 (m, 2H, CH*H*, C'H*H*), 1.58 (bs, J_{PH} = 6.3Hz, 3H, CH_3), 1.42 (d, J_{HH} = 6.8 Hz, 6H, Dipp-CH_3), 1.38 (d, J_{HH} = 6.8 Hz, 6H, Dipp-CH_3), 1.29 (d, J_{HH} = 6.8 Hz, 6H, Dipp-CH_3), 1.23 (d, J_{HH} = 6.8 Hz, 6H, Dipp-CH_3); **^{13}C{^{1}H} NMR** (100.6 MHz, $CDCl_3$, 298 K) δ = 152.1 (dd, J_{PC} = 83.9 Hz, J_{PC} = 30.0 Hz, $C_{carbene}$), 145.7 (ipso-Dipp), 145.3 (ipso-Dipp), 133.3 (d, J_{PC} = 13.8 Hz, *C*CH_3), 132.6 (p-Dipp), 131.1 (o-Dipp), 128.6 (bs, *C*H=*C*H), 125.1 (m-Dipp), 125.0 (m-Dipp), 121.8 (d, J_{PC} = 4.8 Hz, *C*CH_3), 42.9 (dd, , J_{PC} = 42.9 Hz, J_{PC} = 8.1 Hz, N(*C*H_3)$_2$), 37.1 (d, J_{PC} = 36.7 Hz, *C*HH), 29.7-29.5 (several signals, Dipp-*C*H(CH_3)$_2$), 26.0 (Dipp-CH(*C*H_3)$_2$), 25.6 (Dipp-CH(*C*H_3)$_2$), 24.9 (d, J_{PC} = 23.2 Hz, *C'*HH), 22.5-22.3 (m, Dipp-CH(*C*H_3)$_2$), 20.6 (d, J_{PC} = 3.7 Hz, *C*H_3), 19.0 (d, J_{PC} = 2.3 Hz, *C*H_3); **^{31}P{^{1}H} NMR** (162.0 MHz, $CDCl_3$,, 298 K) δ = 65.4 (d, J_{PP} = 227.7 Hz), -41.2 (d, J_{PP} = 230.0 Hz)

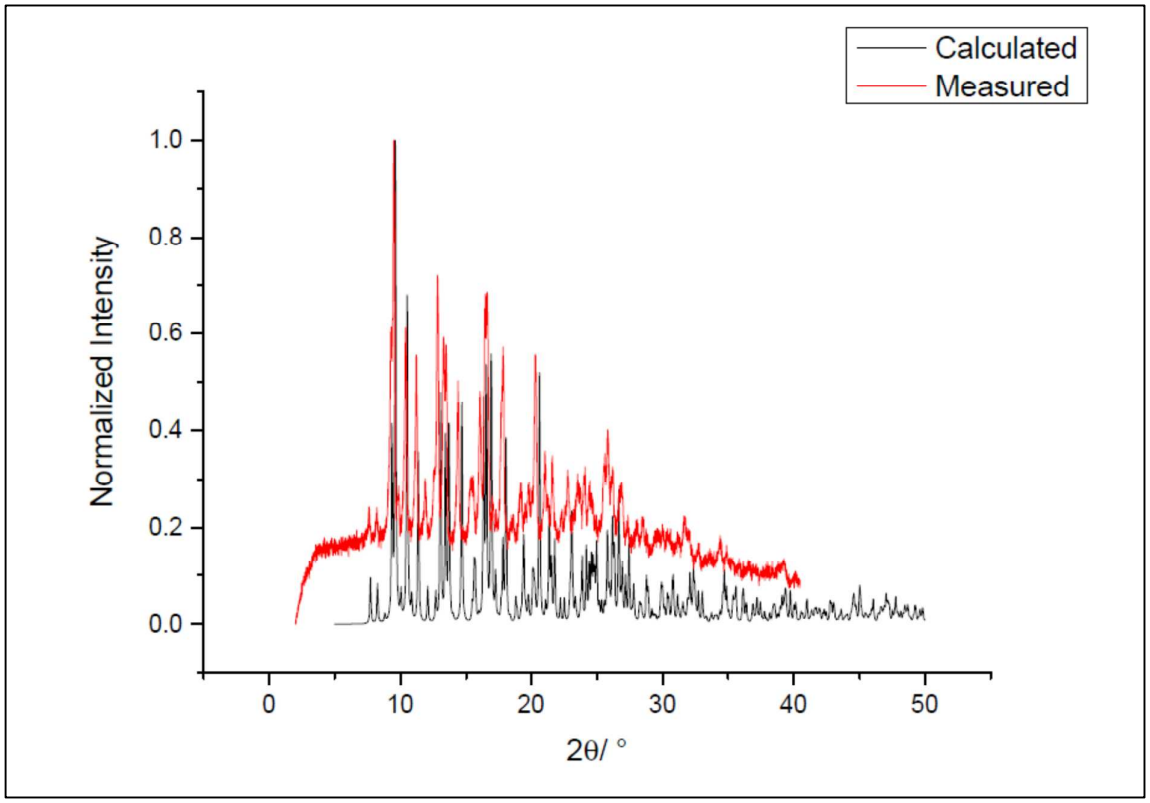

Figure S 9 Calculated and measured powder diffractograms of **4c**

5. Cycloadducts with Cyclopentadiene

Synthesis of Cycloadduct **5a**

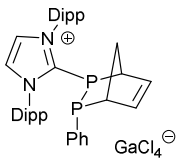

5a

To a solution of **2a** (127.7 mg, 0.227 mmol) in a minimum amount of THF 0.5 mL of cyclopentadiene (ca. 27 eq.) are added followed by the addition of a solution of $GaCl_3$ (40.0 mg, 0.227 mmol, 1.0 eq.) in a minimum amount of hexane over 1 min while stirring at r.t. The obtained orange solution is evaporated *in vacuo* and dissolved in DCM. An unidentified solid is removed by syringe filtration. Covering the obtained yellow solution with hexane and subsequent cooling to -30 °C overnight yields **5a** as pale orange to colourless crystals suitable for x-ray crystallography (54.2 mg, 0.067 mmol, 30 %).

^{1}H NMR (400 MHz, THF-d_8, 298 K) δ = 8.28 (s, 2H, NC*H*=C*H*N), 7.63 (t, J_{HH} = 7.8 Hz, 2H, p-Dipp), 7.58-7.52 (m, 2H, m-Dipp), 7.45-7.40 (m, 2H, m-Dipp), 7.29-7.23 (m, 1H, Ph), 7.18-7.11 (m, 2H, Ph), 6.95-6.88 (m, 2H, Ph), 5.78-5.71 (m, 1H, CC*H*=CHC), 5.62-5.56 (m, 1H, CCH=C*H*C), 3.82-3.69 (m, 1H, PC*H*), 2.92-2.85 (m, 1H, PC'*H*), 2.69 (sept., J_{HH} = 6.8 Hz,

2H, Dipp-C*H*$(CH_3)_2$), 2.57 (sept., J_{HH} = 7.0 Hz, 2H, Dipp-C*H*$(CH_3)_2$), 1.56 (d, J_{HH} = 6.8 Hz, 6H, Dipp-CH_3), 1.32 (d, J_{HH} = 6.9 Hz, 6H, Dipp-CH_3), 1.30 (d, J_{HH} = 7.0 Hz, 6H, Dipp-CH_3), 1.25 (d, J_{HH} = 6.9 Hz, 6H, Dipp-CH_3), not found: methylene-H, regions 1.93-1.77 ppm and 1.45-1.34 ppm show ^{1}H-^{13}C-HSQC crosspeaks to CH_2; **^{13}C{^{1}H} NMR** (100.6 MHz, THF-d_8, 298 K) δ = 145.9 (ipso-Dipp), 145.1 (ipso-Dipp), 139.6 (d, J_{PC} = 12.3 Hz, C*C*=CC), 133.2-132.7 (m, Ph), 132.6 (p-Dipp), 131.5 (o-Dipp), 129.2 (Ph), 128.6 (N*C*H=*C*HN), 127.8-127.6 (m, Ph), 125.4-124.7 (multiple signals, m-Dipp, CC=*C*C), 47.6 (d, J_{PC} = 14.8 Hz, *C*H_2), 46.3 (dd, J_{PC} = 26.9 Hz, J_{PC} = 3.4 Hz, P*C'*H), 43.7 (dd, J_{PC} = 27.5 Hz, J_{PC} = 8.0 Hz, P*C*H), 29.8-29.4 (several signals, *C*H$(CH_3)_2$), 25.3 (Dipp-*C*H_3), 25.1 (Dipp-*C*H_3), 21.6-21.4 (m, Dipp-*C*H_3), 21.2 (Dipp-*C*H_3), not found: $C_{carbene}$, ipso-Ph; **^{31}P{^{1}H} NMR** (162.0 MHz, THF-d_8, 298 K) δ = -13.0 (d, J_{PP} = 240.8 Hz), -15.1 (d, J_{PP} = 242.2 Hz); **^{31}P{^{1}H} NMR** (162.0 MHz, CD_2Cl_2, 298 K) δ = -14.7 (s); impurities observed in NMR

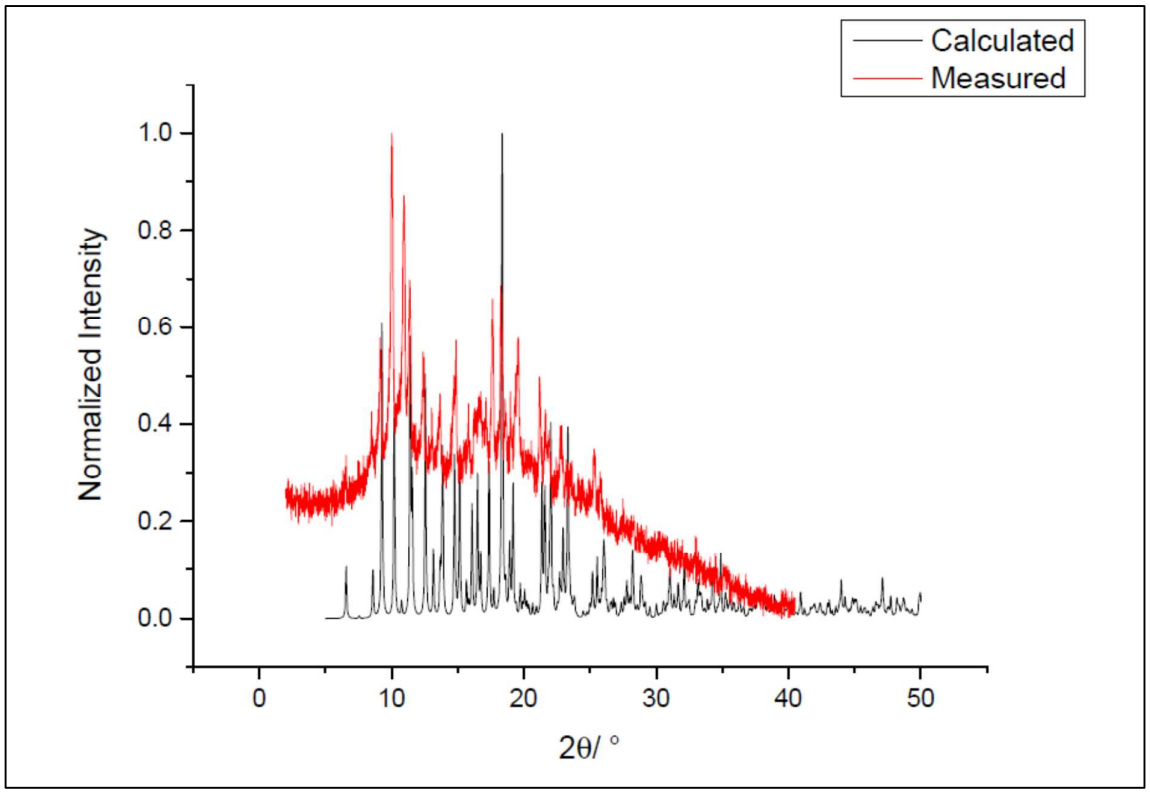

Figure S 10 Calculated and measured powder diffractograms of **5a**

The Reaction of **3b** with Cyclopentadiene – Proof of Reversibility

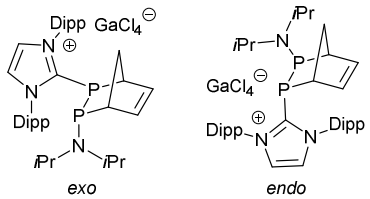

Both diastereomers

In an argon atmosphere, a solution of **2b** (18.8 mg, 0.032 mmol) in 0.5 mL of THF is added to a J. YOUNG type NMR tube containing dry $GaCl_3$ (5.9 mg, 0.034 mmol, 1.06 eq.) yielding a deep orange clear solution. A sealed glass capillary containing 0.85 % D_3PO_4 in D_2O is added as external NMR standard. The 121.5 MHz ^{31}P spectrum (**Figure S 11**a) of this solution shows the signals of **3b** (492.4 ppm, d, J = 520 Hz and 158.3 ppm, d, J = 525 Hz) and the singlet of phosphoric acid at 0 ppm.

Subsequently, cyclopentadiene (0.05 mL, 0.44 mmol, ca. 14 eq.) is added and spectra are recorded directly after the addition (**Figure S 11**b) and 12 h later (c). Both spectra now show two sets of signals in addition to trace signals of **3b** and phosphoric acid. These signals are assigned to the two diastereomers obtained in the [4+2] cycloaddition reaction between **3b** and cyclopentadiene (*cf.* shifts of other cycloaddition products): **5b** (42.5 ppm, d, J = 282 Hz and -24.3 ppm, d, J = 289 Hz) and **5b'** (35.7 ppm, d, J = 279 Hz and -19.0 ppm, d, J = 278 Hz). In the spectrum recorded immediately after the addition of cyclopentadiene, the signals of **5b'** are stronger than the signals of **5b**, while it is the other way round in the spectrum recorded 12 h later (**Figure S 12** shows a magnification). Hence, we assume that **5b'** is the kinetic product isomerising to the thermodynamic product **5b**.

Finally, the solution is carefully evaporated *in vacuo* forming an orange foam, which is left under rotary vane pump vacuum for 1 h. A final NMR spectrum is recorded after the dissolution of the foam in 0.5 mL of THF again showing the signals of **3b** besides traces of the cycloaddition products (**Figure S 11**d).

All 121.5 MHz ^{31}P NMR spectra are recorded with 30 s relaxation delay and apodization is applied (a = 30 Hz).

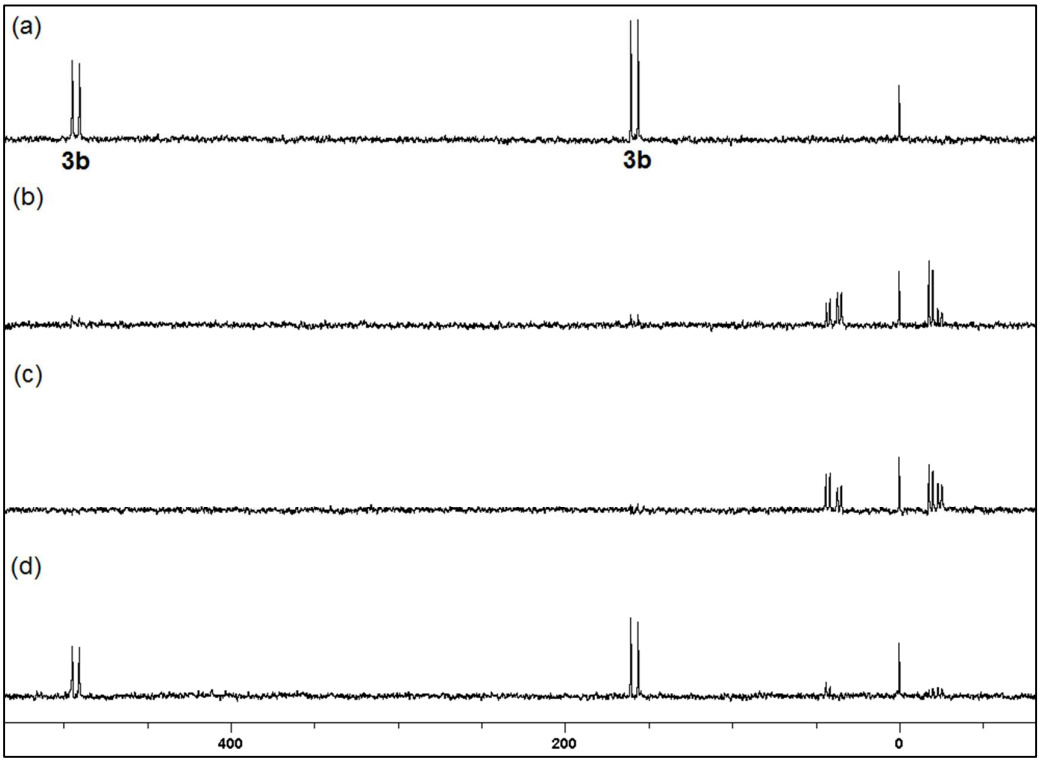

Figure S 11 ^{31}P NMR spectra showing the reversibility of the reaction of cation **3b** with cyclopentadiene. (a) without cyclopentadiene, (b) directly after the addition of cyclopentadiene, (c) 12 h later, (d) after evaporation *in vacuo* and dissolution in THF

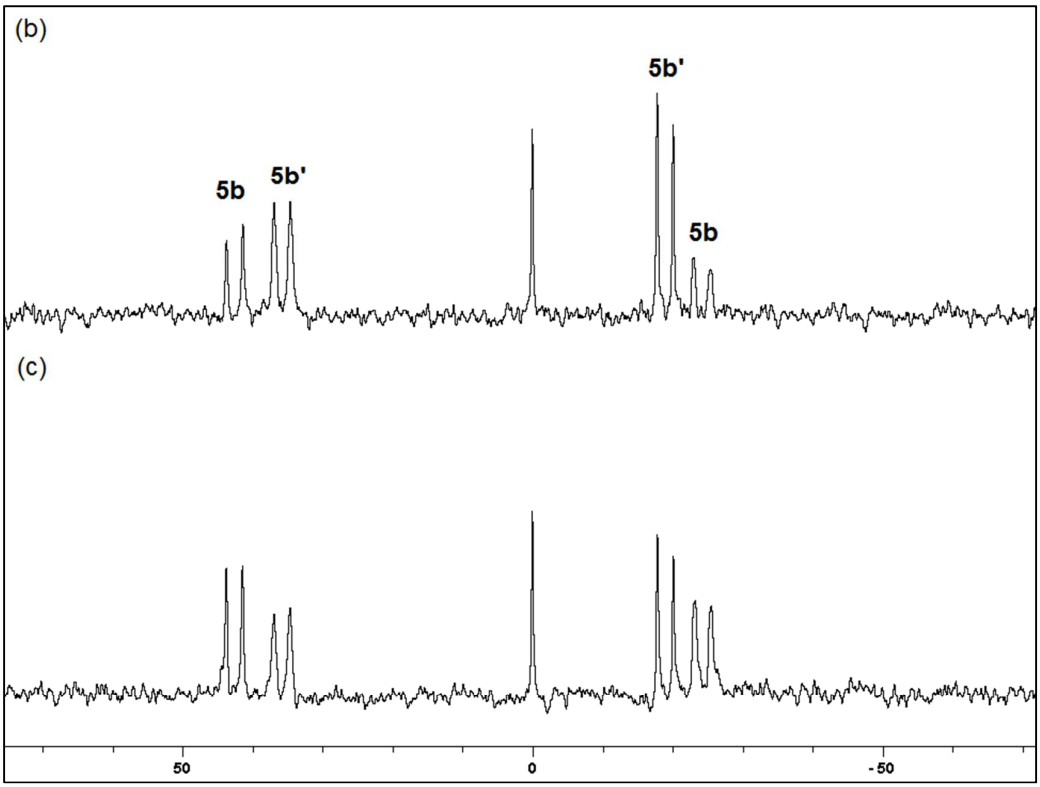

Figure S 12 Detail of the ^{31}P NMR spectrum shown in **Figure S 11**. Spectrum (b) measured directly after the addition of cyclopentadiene, spectrum (c) 12 h later. Two sets of signals are observed, which are assigned to cycloaddition products

Synthesis of Cycloadduct **5c**

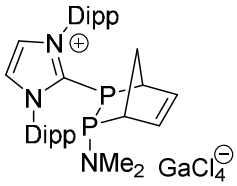

5c

To a solution of **2c** (85.8 mg, 0.162 mmol) and 0.1 mL of cyclopentadiene (ca. 1.2 mmol, 7.5 eq.) in 2 mL of dry THF, a solution of $GaCl_3$ (29.9 mg, 0.170 mmol, 1.05 eq.) in 1 mL of dry hexane is slowly added while stirring. Upon evaporation *in vacuo*, an off-white foam is obtained, which is dissolved in a minimum amount of dry DME. Covering the filtered solution with dry hexane, **5c** is obtained as colourless crystals suitable for XRD (19.1 mg, 0.025 mmol, 15 %). Note that **5c** is extremely sensitive to vacuum as cycloreversion reactions occur. This leads to major impurities, which are observed in NMR spectra (Figure S 14). Therefore, the assignment of NMR signals must be regarded as rough estimation in comparison with similar compounds.

^{1}H NMR (500 MHz, $CDCl_3$, 298 K) δ/ppm = 7.74 (s, 2H, NC*H*=C*H*N), 7.67 (t, J_{HH} = 7.9 Hz, 2H, p-Dipp), 7.49-7.46 (m, 2H, m-Dipp), 7.42-7.37 (m, 2H, m-Dipp), 6.16-6.11 (m, 1H, CC*H*=CHC), 5.52-5.48 (m, 1H, CCH=C*H*C), 3.39-3.25 (m, 1H, PC*H*), 1.74-1.58 (m, 1H, PC*H*), 2.57-2.38 (m, Dipp-C*H*$(CH_3)_2$), 2.14-2.10 (m, 6H, N(CH_3)$_2$), 1.48 (d, J_{HH} = 6.8 Hz, 6H, Dipp-CH_3), 1.35-1.18 (m, Dipp-CH_3), 1.10-1.00 (m, 2H, CH_2); **^{13}C{^{1}H} NMR** (125.8 MHz, $CDCl_3$, 298 K) δ/ppm = 146.0 (ipso-Dipp), 145.2 (ipso-Dipp), 137.9 (d, J_{PC} = 15.6 Hz, C*C*=CC), 132.6 (p-Dipp), 131.5 (o-Dipp), 128.3 (N*C*H=*C*HN), 125.7-124.9 (multiple signals, m-Dipp, CC=*C*C), 48.4 (d, J_{PC} = 39.1 Hz, P*C*H), 44.7-44.4 (m, *C*H_2), 44.0 (dd, J_{PC} = 16.5 Hz, J_{PC} = 6.2 Hz, N(CH_3)$_2$), 29.9-29.2 (several signals, *C*H$(CH_3)_2$), 26.4-22.2 (several signals, Dipp-*C*H_3), not found: $C_{carbene}$, second P*C*H; **^{31}P{^{1}H} NMR** (162.0 MHz, $CDCl_3$, 298 K) δ/ppm = 66.5 (d, J_{PP} = 258.6 Hz), -25.2 (d, J_{PP} = 258.3 Hz), beside major impurities

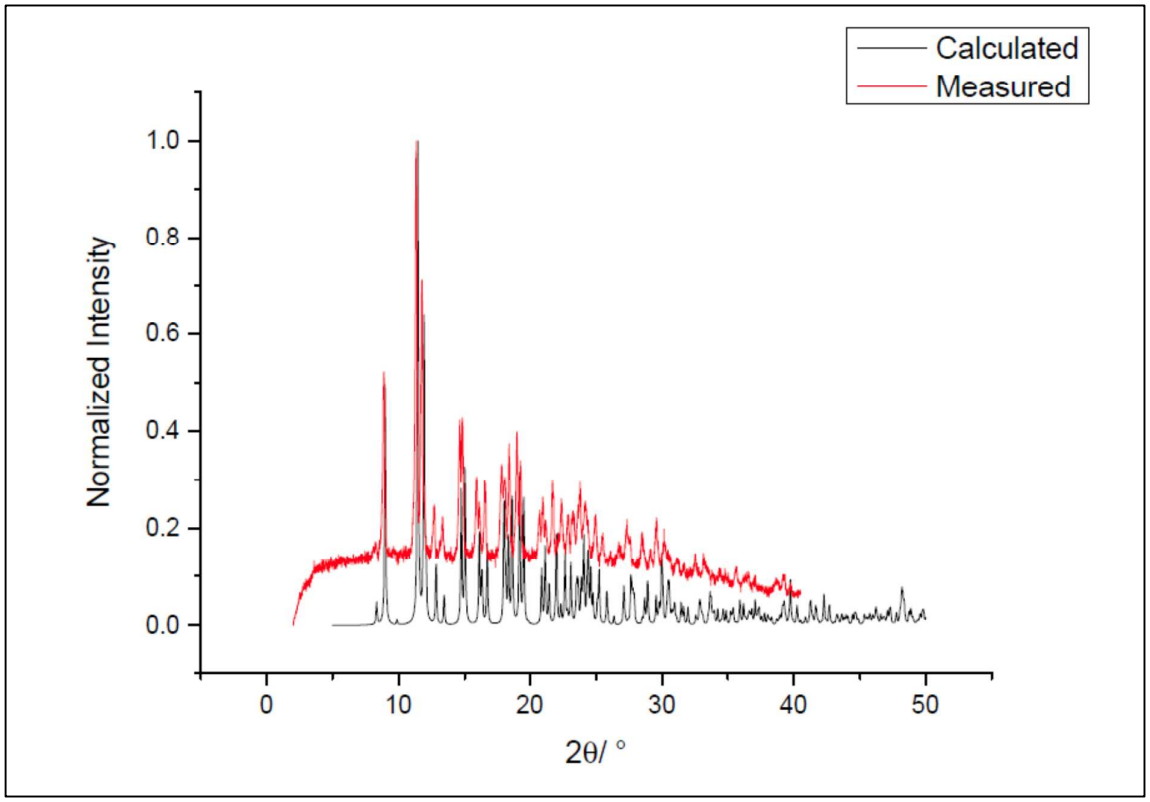

Figure S 13 Calculated and measured powder diffractograms of **5c**

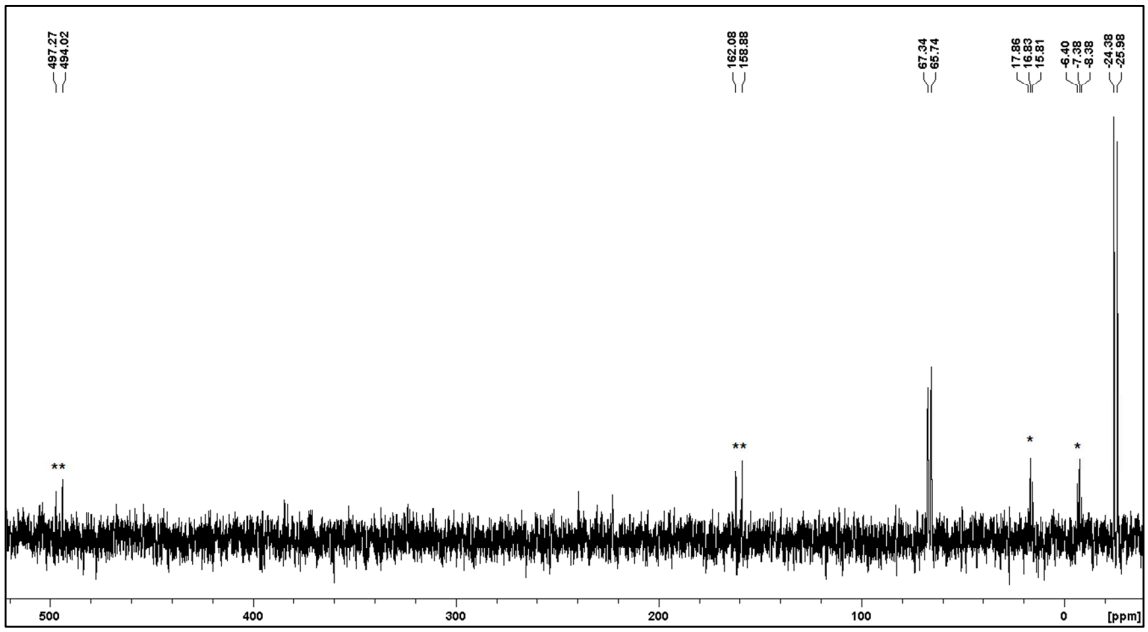

Figure S 14 162.0 MHz $^{31}P\{^{1}H\}$ NMR spectrum of **5c**. Beside the signals of **5c**, signals assigned to **(3c)$_2$** (*) and the monomeric cation **3c** (**), which has not been observed otherwise, are detected

Crystallographic Tables

Table S 1 Crystal data and structure refinement for **2a** 23
Table S 2 Crystal data and structure refinement for **2b** 24
Table S 3 Crystal data and structure refinement for **3b** 25
Table S 4 Crystal data and structure refinement for **(3c)$_2$** 26
Table S 5 Crystal data and structure refinement for **4a** 27
Table S 6 Crystal data and structure refinement for **4b** 28
Table S 7 Crystal data and structure refinement for **4c** 29
Table S 8 Crystal data and structure refinement for **5a** 30
Table S 9 Crystal data and structure refinement for **5c** 31

Table S 1 Crystal data and structure refinement for **2a**

CCDC number	1415566
Empirical formula	$C_{33}H_{41}N_2P_2Cl$
Formula weight	563.07
Temperature/K	102.0
Crystal system	monoclinic
Space group	$P2_1/n$
a/Å	10.0682(3)
b/Å	12.4824(3)
c/Å	24.4361(6)
α/°	90
β/°	93.0570(10)
γ/°	90
Volume/Å^3	3066.64(14)
Z	4
ρ_{calc}g/cm^3	1.220
μ/mm^{-1}	2.262
F(000)	1200.0
Crystal size/mm^3	0.19 × 0.164 × 0.097
Radiation	CuKα (λ = 1.54178)
2Θ range for data collection/°	7.246 to 157.984
Index ranges	$-12 \leq h \leq 12$, $-15 \leq k \leq 15$, $-31 \leq l \leq 31$
Reflections collected	65434
Independent reflections	6607 [R_{int} = 0.0581, R_{sigma} = 0.0270]
Data/restraints/parameters	6607/0/351
Goodness-of-fit on F^2	1.074
Final R indexes [I>=2σ (I)]	R_1 = 0.0445, wR_2 = 0.1129
Final R indexes [all data]	R_1 = 0.0513, wR_2 = 0.1175
Largest diff. peak/hole / e Å^{-3}	0.53/-0.35

Table S 2 Crystal data and structure refinement for **2b**

CCDC	1415567
Empirical formula	$C_{33}H_{50}N_3P_2Cl$
Formula weight	586.15
Temperature/K	100.0
Crystal system	triclinic
Space group	P-1
a/Å	10.4571(2)
b/Å	10.8862(2)
c/Å	16.6912(3)
α/°	83.6921(8)
β/°	82.8084(8)
γ/°	62.1884(8)
Volume/Å^3	1664.52(5)
Z	2
ρ_{calc}g/cm^3	1.169
μ/mm^{-1}	0.236
F(000)	632.0
Crystal size/mm^3	0.297 × 0.176 × 0.083
Radiation	MoKα (λ = 0.71073)
2Θ range for data collection/°	2.464 to 54.228
Index ranges	$-13 \leq h \leq 13$, $-10 \leq k \leq 13$, $-21 \leq l \leq 21$
Reflections collected	25555
Independent reflections	7359 [R_{int} = 0.0346, R_{sigma} = 0.0483]
Data/restraints/parameters	7359/0/364
Goodness-of-fit on F^2	1.032
Final R indexes [I>=2σ (I)]	R_1 = 0.0399, wR_2 = 0.0792
Final R indexes [all data]	R_1 = 0.0592, wR_2 = 0.0867
Largest diff. peak/hole / e Å^{-3}	0.37/-0.29

Table S 3 Crystal data and structure refinement for **3b**

CCDC	1415568
Empirical formula	$C_{33}H_{50}Cl_4GaN_3P_2$
Formula weight	762.22
Temperature/K	100.0
Crystal system	monoclinic
Space group	$P2_1/c$
a/Å	10.3933(8)
b/Å	24.7035(17)
c/Å	15.9464(12)
α/°	90
β/°	105.836(4)
γ/°	90
Volume/Å^3	3938.9(5)
Z	4
ρ_{calc}g/cm^3	1.285
μ/mm^{-1}	1.077
F(000)	1592.0
Crystal size/mm^3	0.185 × 0.132 × 0.083
Radiation	MoKα (λ = 0.71073)
2Θ range for data collection/°	3.126 to 52.742
Index ranges	$-12 \leq h \leq 12$, $-30 \leq k \leq 30$, $-19 \leq l \leq 19$
Reflections collected	51773
Independent reflections	8040 [R_{int} = 0.0423, R_{sigma} = 0.0319]
Data/restraints/parameters	8040/0/421
Goodness-of-fit on F^2	1.025
Final R indexes [I>=2σ (I)]	R_1 = 0.0343, wR_2 = 0.0708
Final R indexes [all data]	R_1 = 0.0511, wR_2 = 0.0769
Largest diff. peak/hole / e Å^{-3}	0.67/-0.54

Table S 4 Crystal data and structure refinement for **(3c)$_2$**

CCDC	1415569
Empirical formula	$C_{62}H_{94}Cl_8Ga_2N_6O_2P_4$
Formula weight	1502.35
Temperature/K	100
Crystal system	orthorhombic
Space group	Pbcn
a/Å	32.9377(6)
b/Å	23.6356(4)
c/Å	19.1985(4)
α/°	90
β/°	90
γ/°	90
Volume/Å^3	14946.1(5)
Z	8
ρ_{calc}g/cm^3	1.335
μ/mm^{-1}	1.136
F(000)	6256.0
Crystal size/mm^3	0.452 × 0.224 × 0.222
Radiation	MoKα (λ = 0.71073)
2Θ range for data collection/°	3.686 to 61.102
Index ranges	$-47 \leq h \leq 38$, $-33 \leq k \leq 33$, $-27 \leq l \leq 13$
Reflections collected	103106
Independent reflections	22865 [R_{int} = 0.0493, R_{sigma} = 0.0449]
Data/restraints/parameters	22865/155/895
Goodness-of-fit on F^2	1.017
Final R indexes [I>=2σ (I)]	R_1 = 0.0427, wR_2 = 0.0893
Final R indexes [all data]	R_1 = 0.0755, wR_2 = 0.1023
Largest diff. peak/hole / e Å^{-3}	0.51/-0.67

Table S 5 Crystal data and structure refinement for **4a**

CCDC	1415570
Empirical formula	$C_{39}H_{51}N_2P_2Cl_4Ga$
Formula weight	821.28
Temperature/K	101.1
Crystal system	monoclinic
Space group	$P2_1/c$
a/Å	10.5864(5)
b/Å	16.4856(8)
c/Å	24.2540(11)
α/°	90
β/°	102.366(2)
γ/°	90
Volume/Å^3	4134.7(3)
Z	4
ρ_{calc}g/cm^3	1.319
μ/mm^{-1}	1.030
F(000)	1712.0
Crystal size/mm^3	0.992 × 0.541 × 0.526
Radiation	MoKα (λ = 0.71073)
2Θ range for data collection/°	4.642 to 61.126
Index ranges	$-15 \leq h \leq 15$, $-23 \leq k \leq 23$, $-34 \leq l \leq 34$
Reflections collected	78415
Independent reflections	12547 [R_{int} = 0.0763, R_{sigma} = 0.0426]
Data/restraints/parameters	12547/0/443
Goodness-of-fit on F^2	1.081
Final R indexes [I>=2σ (I)]	R_1 = 0.0432, wR_2 = 0.0859
Final R indexes [all data]	R_1 = 0.0592, wR_2 = 0.0917
Largest diff. peak/hole / e Å^{-3}	0.83/-0.49

Table S 6 Crystal data and structure refinement for **4b**

CCDC	1415571
Empirical formula	$C_{39}H_{60}N_3P_2Cl_4Ga$
Formula weight	844.36
Temperature/K	100
Crystal system	monoclinic
Space group	$P2_1/c$
a/Å	10.7703(2)
b/Å	15.0762(3)
c/Å	27.5758(5)
α/°	90
β/°	101.0720(10)
γ/°	90
Volume/Å^3	4394.28(14)
Z	4
ρ_{calc}g/cm^3	1.276
μ/mm^{-1}	0.972
F(000)	1776.0
Crystal size/mm^3	0.297 × 0.255 × 0.15
Radiation	MoKα (λ = 0.71073)
2Θ range for data collection/°	4.044 to 52.744
Index ranges	$-13 \leq h \leq 5$, $-18 \leq k \leq 18$, $-34 \leq l \leq 34$
Reflections collected	34737
Independent reflections	8936 [R_{int} = 0.0272, R_{sigma} = 0.0290]
Data/restraints/parameters	8936/0/461
Goodness-of-fit on F^2	1.037
Final R indexes [I>=2σ (I)]	R_1 = 0.0363, wR_2 = 0.0908
Final R indexes [all data]	R_1 = 0.0487, wR_2 = 0.0981
Largest diff. peak/hole / e Å^{-3}	0.85/-0.37

Table S 7 Crystal data and structure refinement for **4c**

CCDC	1415572
Empirical formula	$C_{35}H_{52}N_3P_2Cl_4Ga$
Formula weight	788.25
Temperature/K	100
Crystal system	orthorhombic
Space group	Pbca
a/Å	20.036(3)
b/Å	18.337(2)
c/Å	21.409(3)
α/°	90
β/°	90
γ/°	90
Volume/Å^3	7865.6(18)
Z	8
ρ_{calc}g/cm^3	1.331
μ/mm^{-1}	1.081
F(000)	3296.0
Crystal size/mm^3	0.396 × 0.32 × 0.264
Radiation	MoKα (λ = 0.71073)
2Θ range for data collection/°	3.562 to 58.374
Index ranges	$-27 \leq h \leq 27$, $-24 \leq k \leq 20$, $-29 \leq l \leq 29$
Reflections collected	55940
Independent reflections	10591 [R_{int} = 0.0281, R_{sigma} = 0.0224]
Data/restraints/parameters	10591/18/464
Goodness-of-fit on F^2	1.199
Final R indexes [I>=2σ (I)]	R_1 = 0.0411, wR_2 = 0.1456
Final R indexes [all data]	R_1 = 0.0504, wR_2 = 0.1520
Largest diff. peak/hole / e Å^{-3}	0.85/-0.52

Table S 8 Crystal data and structure refinement for **5a**

CCDC	1415573
Empirical formula	$C_{38}H_{47}Cl_4GaN_2P_{2.07}$
Formula weight	807.32
Temperature/K	100
Crystal system	monoclinic
Space group	$P2_1/c$
a/Å	10.4962(7)
b/Å	16.4244(11)
c/Å	23.8724(15)
α/°	90
β/°	101.7157(11)
γ/°	90
Volume/Å^3	4029.7(5)
Z	4
ρ_{calc}g/cm^3	1.331
μ/mm^{-1}	1.059
F(000)	1676.0
Crystal size/mm^3	0.49 × 0.34 × 0.2
Radiation	MoKα (λ = 0.71073)
2Θ range for data collection/°	3.03 to 58.438
Index ranges	$-14 \leq h \leq 14$, $-22 \leq k \leq 22$, $-32 \leq l \leq 32$
Reflections collected	44260
Independent reflections	10899 [R_{int} = 0.0312, R_{sigma} = 0.0287]
Data/restraints/parameters	10899/0/440
Goodness-of-fit on F^2	1.046
Final R indexes [I>=2σ (I)]	R_1 = 0.0371, wR_2 = 0.0915
Final R indexes [all data]	R_1 = 0.0472, wR_2 = 0.0970
Largest diff. peak/hole / e Å^{-3}	0.72/-0.40

Table S 9 Crystal data and structure refinement for **5c**

CCDC	1415574
Empirical formula	$C_{34}H_{48}N_3P_2Cl_4Ga$
Formula weight	772.21
Temperature/K	100
Crystal system	monoclinic
Space group	Cc
a/Å	19.7393(3)
b/Å	13.1426(2)
c/Å	16.1564(2)
α/°	90
β/°	115.0700(10)
γ/°	90
Volume/Å^3	3796.52(10)
Z	4
ρ_{calc}g/cm^3	1.351
μ/mm^{-1}	1.118
F(000)	1608.0
Crystal size/mm^3	0.331 × 0.125 × 0.094
Radiation	MoKα (λ = 0.71073)
2Θ range for data collection/°	3.846 to 66.186
Index ranges	$-30 \leq h \leq 30$, $-19 \leq k \leq 20$, $-23 \leq l \leq 22$
Reflections collected	24678
Independent reflections	11114 [R_{int} = 0.0340, R_{sigma} = 0.0684]
Data/restraints/parameters	11114/28/431
Goodness-of-fit on F^2	0.953
Final R indexes [I>=2σ (I)]	R_1 = 0.0371, wR_2 = 0.0731
Final R indexes [all data]	R_1 = 0.0464, wR_2 = 0.0764
Largest diff. peak/hole / e Å^{-3}	0.75/-0.29

References

1. A. M. Tondreau, Z. Benko, J. R. Harmer and H. Grützmacher, *Chemical Science*, 2014, **5**, 1545-1554.
2. F. F. Puschmann, D. Stein, D. Heift, C. Hendriksen, Z. A. Gal, H.-F. Grützmacher and H. Grützmacher, *Angewandte Chemie International Edition*, 2011, **50**, 8420-8423.
3. D. Heift, Z. Benko and H. Grützmacher, *Dalton Transactions*, 2014, **43**, 831-840.
4. P. Tang, W. Wang and T. Ritter, *Journal of the American Chemical Society*, 2011, **133**, 11482-11484.
5. E. J. Nurminen, J. K. Mattinen and H. Lonnberg, *Journal of the Chemical Society, Perkin Transactions 2*, 1998, DOI: 10.1039/A801250D, 1621-1628.
6. U. Berens, U. Englert, S. Geyser, J. Runsink and A. Salzer, *European Journal of Organic Chemistry*, 2006, **2006**, 2100-2109.
7. O. V. Dolomanov, L. J. Bourhis, R. J. Gildea, J. A. K. Howard and H. Puschmann, *Journal of Applied Crystallography*, 2009, **42**, 339-341.

Table of Contents for DT-ART-08-2015-003014

From the Parent Phosphinidene-Carbene Adduct NHC=PH to Cationic P_4-Rings and P_2-Cycloaddition Products

*Andreas Beil,[a] Robert J. Gilliard, Jr.,[a] Hansjörg Grützmacher[a]**

[a] Laboratory of Inorganic Chemistry, ETH Zürich, Vladimir-Prelog-Weg 1, 8093 Zürich, Switzerland.
E-mail: hgruetzmacher@ethz.ch

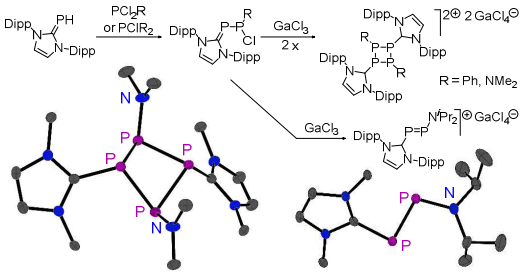

The parent phosphinidene-carbene adduct NHC=PH reacts with chlorophosphanes yielding NHC-supported chlorodiphosphanes, which can be transformed to novel P_4-rings and reactive 1,2-diphosphenes.